Aeolian Islands

http://www.decadevolcano.net/photos/europe/stromboli/stromboli_0903/stromboli_36222.jpg


APAT
Agenzia per la Protezione dell'Ambiente e per i Servizi Tecnici
Dipartimento Difesa del Suolo
Servizio Geologico d'Italia
GEOLOGICAL MAP OF ITALY
1:1 250 000 Scale
MAIN TECTONO-STRATIGRAPHIC UNITS
SPECIALLY PRINTED FOR THE 32nd INTERNATIONAL GEOLOGICAL CONGRESS
ITALIA 2004

Three Volcanic Regions

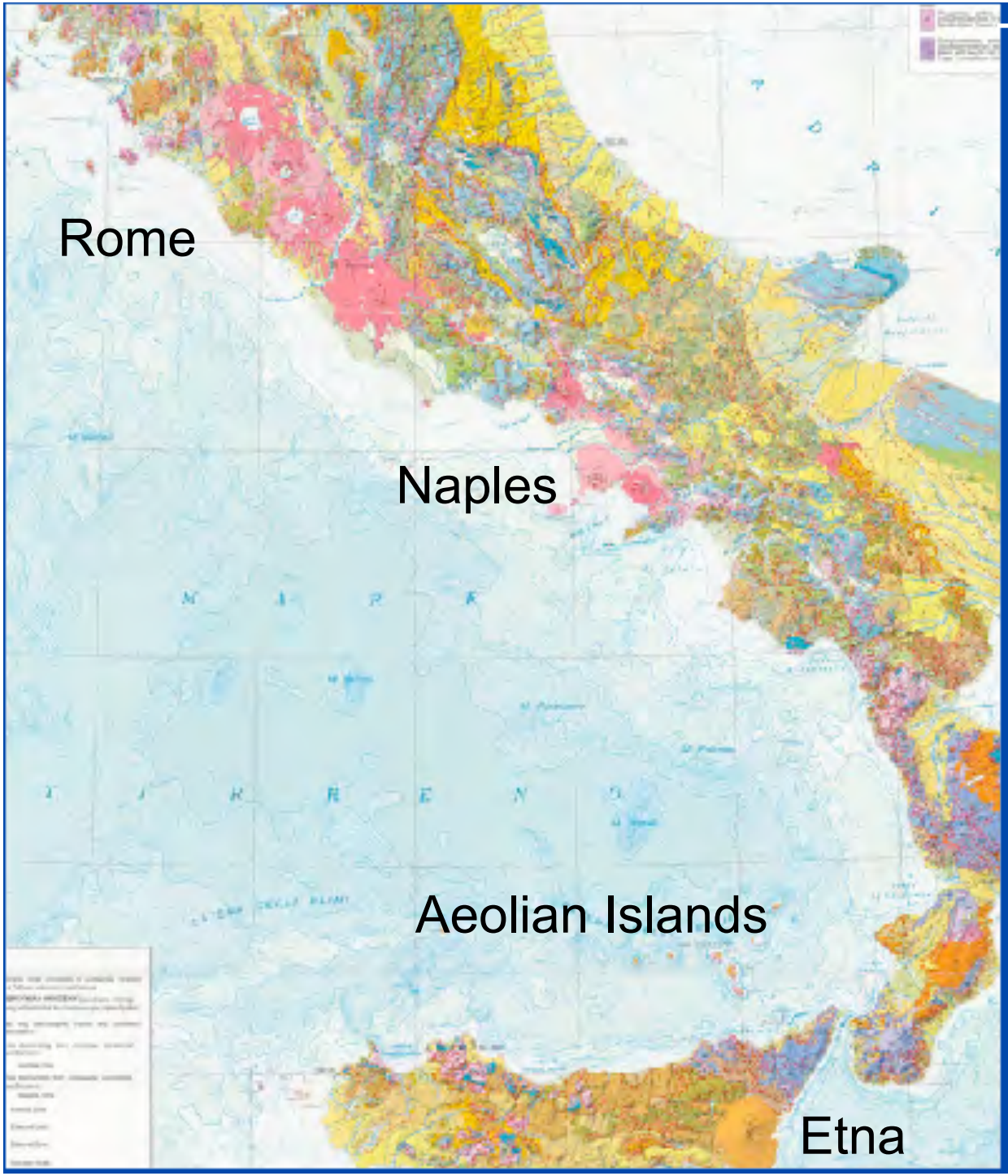

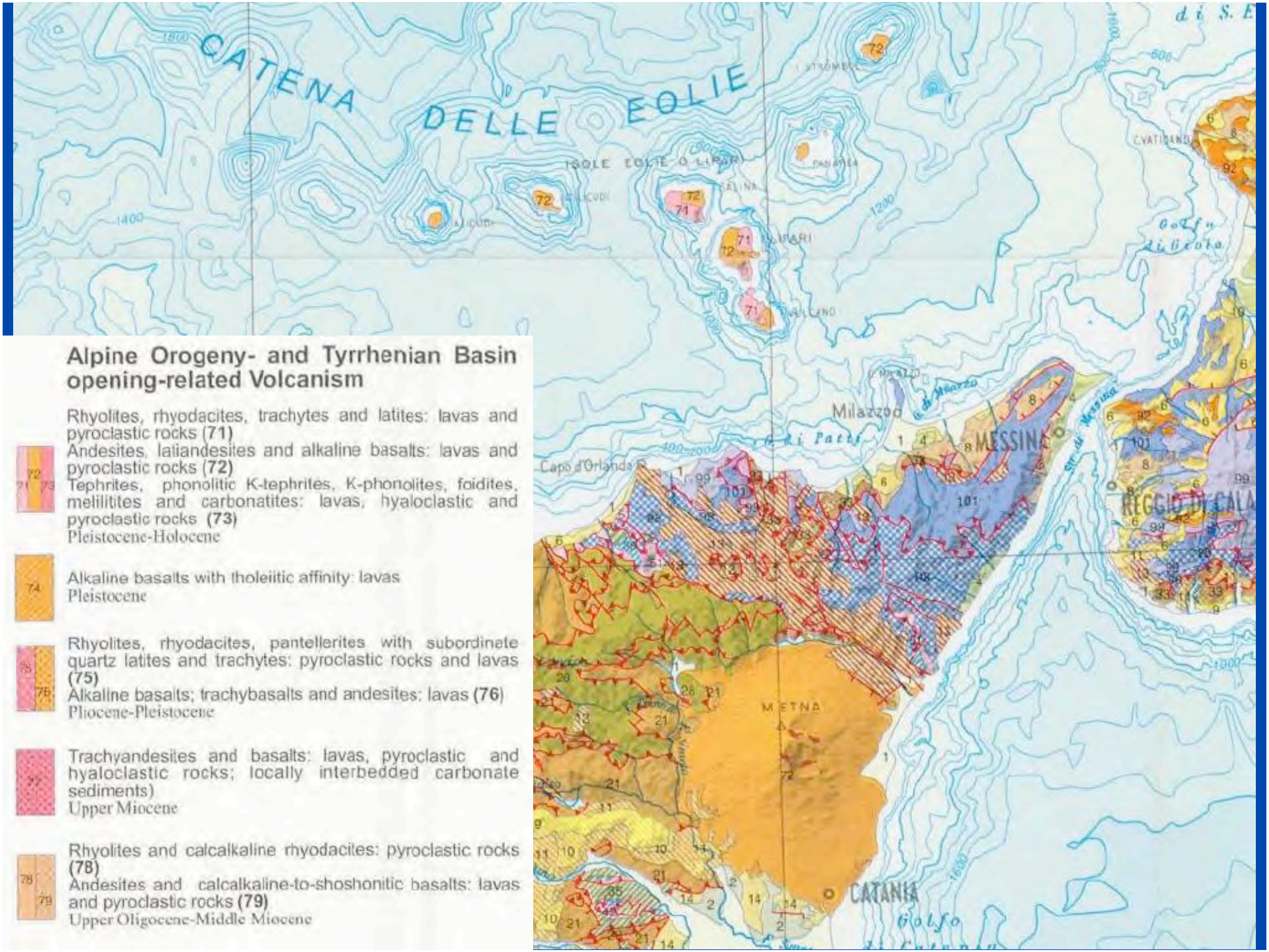
CATENA DELLE EOLIE
ISOLE EOLIE O LIPARI
Milazzo
MESSINA
REGGIO DI CALA
METNA
CATANIA
Golfo di Patti
Capo d'Orlando
Golfo di Gioia
Alpine Orogeny- and Tyrrhenian Basin opening-related Volcanism
Rhyolites, rhyodacites, trachytes and latites: lavas and pyroclastic rocks (71)
Andesites, latiandesites and alkaline basalts: lavas and pyroclastic rocks (72)
Tephrites, phonolitic K-tephrites, K-phonolites, foidites, melilitites and carbonatites: lavas, hyaloclastic and pyroclastic rocks (73)
Pleistocene-Holocene
Alkaline basalts with tholeiitic affinity: lavas
Pleistocene
Rhyolites, rhyodacites, pantellerites with subordinate quartz latites and trachytes: pyroclastic rocks and lavas (75)
Alkaline basalts; trachybasalts and andesites: lavas (76)
Pliocene-Pleistocene
Trachyandesites and basalts: lavas, pyroclastic and hyaloclastic rocks; locally interbedded carbonate sediments)
Upper Miocene
Rhyolites and calcalkaline rhyodacites: pyroclastic rocks (78)
Andesites and calcalkaline-to-shoshonitic basalts: lavas and pyroclastic rocks (79)
Upper Oligocene-Middle Miocene

ISS017E009545

ISS024E009908

Aeolian Islands

http://eol.jsc.nasa.gov/

ISS006E43151

Stromboli Island

http://eol.jsc.nasa.gov/

ISS027E028732

Vulcano Island

http://eol.jsc.nasa.gov/

ISS027E028726

Lipari

http://eol.jsc.nasa.gov/

http://www.flickr.com/photos/grafwilliam/697535448/sizes/o/in/photostream/

Stromboili, Aeolian Islands

http://www.ingv.it/vulcani/stromboli/

http://www.ingv.it/vulcani/stromboli/

http://www.ingv.it/vulcani/stromboli/

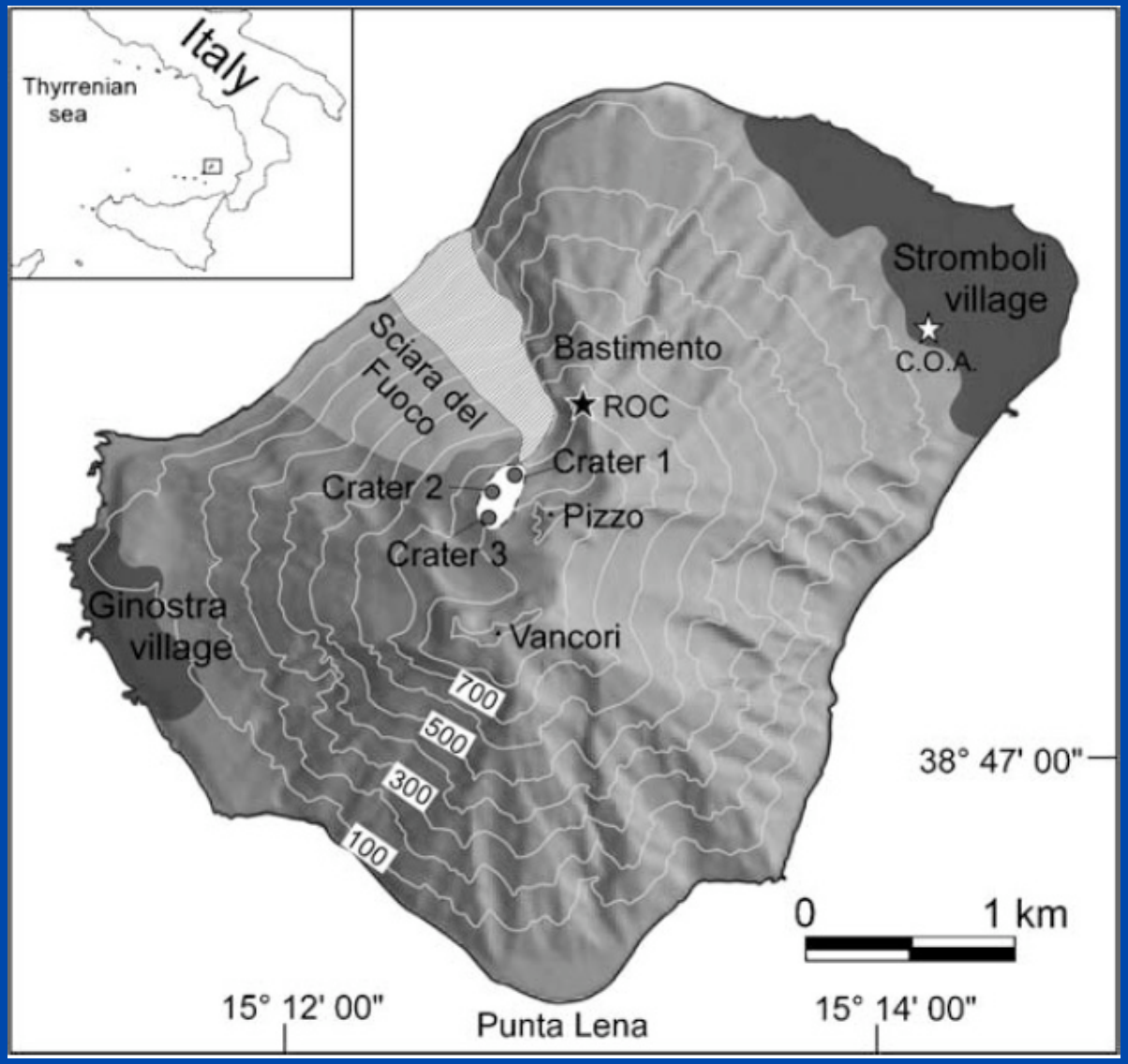

Rossi et al 2006

April 5, 2003

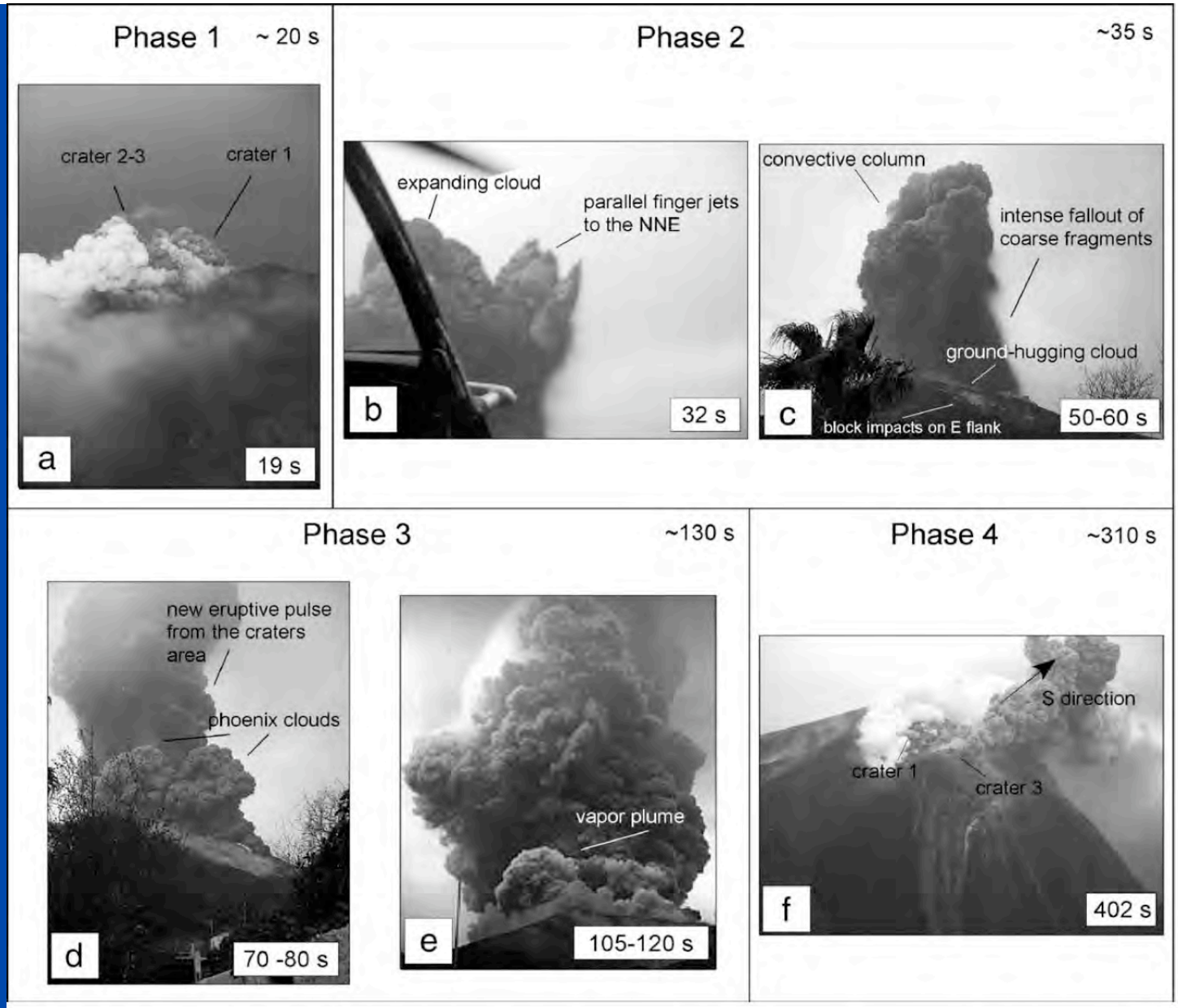

g. 2. Pictures of the April 5 eruption. (a) Red ash plume emitted from crater 3 during late Phase 1. (b) Main blast showing ballistic blocks ejected to NNE and expanding ash cloud during early Phase 2. (c) Vertical column rising above the crater area and formation of pyroclastic flow during early ase 3. (d) Phoenix clouds rising above the Bastimento area. (e) Vapor plume replacing the phoenix cloud during late Phase 3. (f) Vapor plume and plumes emitted from crater 3 during late Phase 4. Pictures in a, b, and f are from S. Calvari in [10], times in the lower right indicate relative times recorded by digital camera; picture c is from A. Franssen, and pictures d and e are from S. Ballarò.

Rossi et al 2006

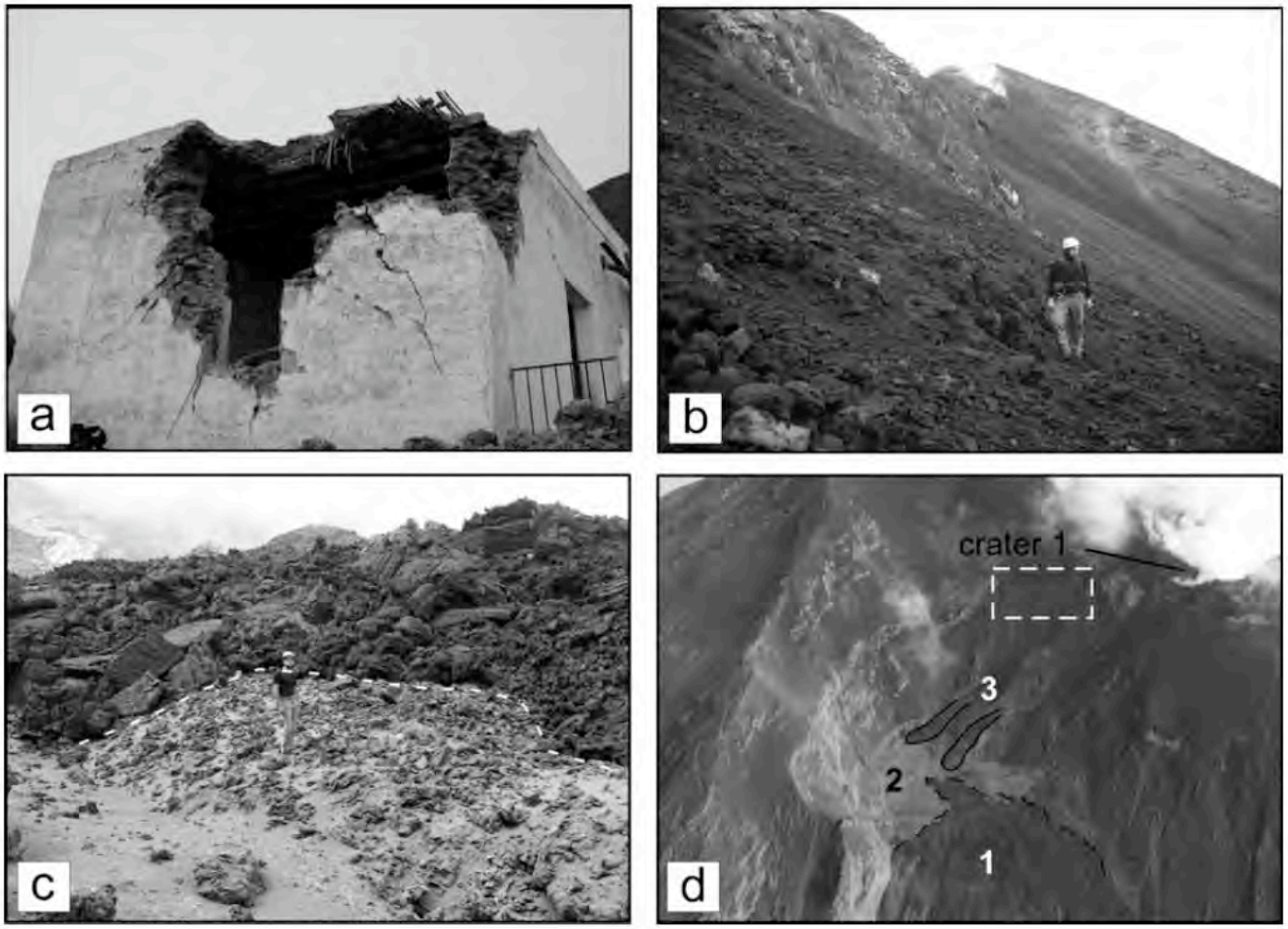

Fig. 4. Pictures of the deposits of the eruption. (a) House in Ginostra village damaged by m-sized block ejected during Phase 2. (b) Proximal fallout layer along the scarp connecting crater 1 to the Sciara del Fuoco. (c) Scoria flow deposit in active lava field partly covered by younger lava flows. Note ash covering the flow deposit. (d) Active lava flows (1) covering deposits of pyroclastic flows (2), photographed on April 18, 2003. Hot avalanche lobes (3) overlap the scoria flow deposit on northern side of the lava field. White box encloses proximal fallout area photographed in picture (b). Picture (a) is courtesy of K. Cashman.

Rossi et al 2006

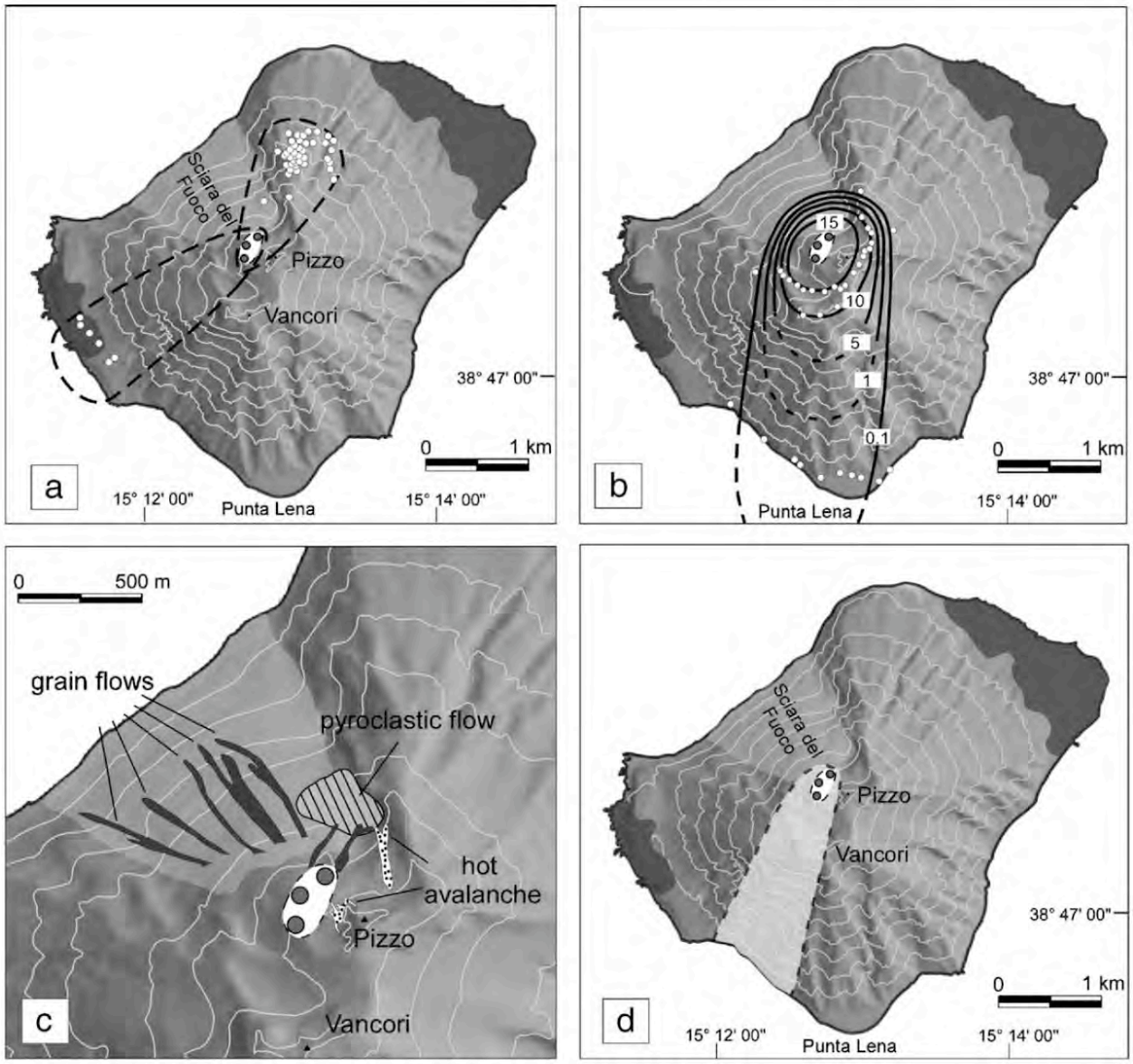

Fig. 5. (a) Mapped impact craters from larger ballistic blocks emitted during Phase 2. Dashed lines enclose the areas of higher concentration of blocks. Measurements of blocks and GPS locations of 16 impact craters were performed during field surveys made in April and May 2003. Impact craters produced by blocks with diameter ≥2 m were also mapped using data aerial photogrammetric surveys of the island (March 15, 2003, scale 1: 7000; April 16 scale 1: 8000 and May 26, 2003, scale 1: 5000) [16]. (b) Isomass map of fallout deposit. Values refer to kg/m^2. (c) Areal dispersion of grain flow (dark gray), hot avalanche (dottled area) and pyroclastic flow (striped area) deposits. (d) Dispersion of top ash layer.

Rossi et al 2006

Fig. 1 Aerial view of Stromboli island from NE with

Rossi et al 2000

Trench 1 (NE sector- 500 m a.s.l.)

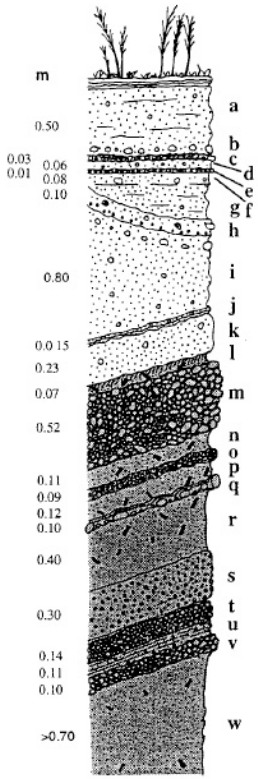

a- reworked coarse ash with scattered pumiceous lapilli
b- pumiceous bombs (Φmax 10 cm)
c- pumiceous lapilli and bombs (Φmax 10 cm) and minor scoriaceous lapilli, with cohesive reddish ash; rare lithics of oxidized lavas (Φmax 10 cm)
d- coarse ash with abundant red lithics and scattered pumiceous lapilli (Φmax 5 cm)
e- pumiceous and scoriaceous lapilli with cohesive reddish-brown ash
f- pumiceous lapilli (Φmax 5 cm)
g- reworked, cross-stratified coarse ash with scattered pumiceous lapilli
h- coarse ash with scattered pumiceous lapilli in the uppermost part; red ash with scattered pumiceous lapilli at the base
i- massive bed of reworked coarse ash with scattered pumiceous lapilli
j- coarse ash and pumiceous lapilli; thin layer of red fine ash at the very base
k- crudely stratified, reworked, coarse ash with scattered pumiceous lapilli and bombs
l- humified red-brown ash layer embedding cm-sized charcoal fragments (paleosol)
m-scoriaceous lapilli (Φmax 8 cm) and minor oxidized lava clasts (Φmax 5 cm)
n- reworked coarse ash with small charcoals
o- scoriaceous lapilli (Φmax 7 cm)
p- crudely stratified, reworked, coarse ash and lapilli with small charcoals
q- poorly vesicular bombs (Φmax 21 cm)
r- massive bed of reworked coarse ash with small charcoals
s- partially reworked air-fall bed of coarse ash and lapilli
t- coarse ash and fine lapilli (Φmax 6 cm) topped by thin layers of grey and red fine-ash
u- alternating reworked layers of coarse ash and fine lapilli
v- scoriaceous lapilli
w-reworked coarse ash with small charcoals

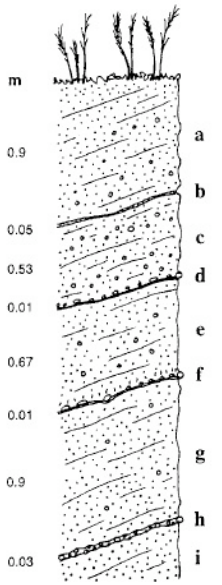

Trench 2 (NE sector - 450 m a.s.l.)

a- crudely stratified reworked coarse ash with scattered pumiceous lapilli
b- fine ash with scattered fine pumiceous lapilli
c- crudely stratified reworked coarse ash with scattered pumiceous lapilli
d- pumiceous lapilli and bombs (Φmax 9 cm) and minor black scoriaceous lapilli. Thin reddish-brown fine ash layer at the very base
e- crudely stratified reworked coarse ash with scattered pumiceous lapilli
f- pumiceous lapilli and bombs (Φmax 11 cm) and minor scoriaceous lapilli; thin reddish-brown accretionary-lapilli rich, fine-ash layer at the very base
g- vaguely stratified reworked coarse ash with scattered pumiceous lapilli
h- pumiceous lapilli (Φmax 5 cm)
i- reworked coarse ash

Table 2 Chemical analyses of the products of the upper and lower sequences and of the 23 August 1998 explosion

Lower sequence						23 August 1998	
Sample	ST68	ST70	ST74	ST89	ST90	ST140	ST133
Layer	Scoria m	Scoria o	Scoria q	Scoria t	Scoria v	Pumice	Scoria
SiO_2	52.24	53.98	51.94	52.07	52.94	49.05	49.89
TiO_2	0.80	0.84	0.82	0.77	0.81	0.97	0.98
Al_2O_3	18.05	17.75	17.94	17.36	18.03	17.14	18.05
Fe_2O_3	2.82	3.16	4.03	2.89	3.24	4.60	3.86
FeO	5.10	4.55	4.24	4.79	4.72	4.40	4.90
MnO	0.15	0.15	0.15	0.15	0.15	0.16	0.16
MgO	5.99	5.11	5.74	7.38	5.38	6.93	5.97
CaO	9.83	8.81	10.12	9.78	9.37	11.59	10.78
Na_2O	2.38	2.58	2.35	2.09	2.25	2.38	2.60
K_2O	1.61	1.96	1.49	1.58	1.81	1.62	2.07
P_2O_5	0.25	0.26	0.22	0.20	0.23	0.42	0.45
LOI	0.78	0.86	0.94	0.94	1.07	0.73	0.28

Upper sequence										
Trench 1						Trench 2				
Sample	ST61	ST62	ST63	ST64	ST65	ST82	ST82	ST79	ST79	ST81
Layer	Pumice c	Pumice e	Pumice f	Pumice h top	Pumice h bottom	Pumice d	Scoria d	Pumice f	Scoria f	Pumice h
SiO_2	51.36	51.57	51.25	52.60	52.80	50.87	51.07	51.35	52.50	51.55
TiO_2	0.90	0.91	0.91	1.00	0.99	0.90	0.90	0.87	0.84	0.87
Al_2O_3	16.45	16.75	16.00	17.31	17.75	16.56	17.13	16.62	16.81	16.20
Fe_2O_3	3.09	2.82	3.84	3.94	3.12	3.46	3.10	3.00	3.13	3.01
FeO	5.21	5.38	4.94	4.75	5.27	5.11	5.18	5.08	4.76	5.40
MnO	0.15	0.15	0.16	0.16	0.15	0.16	0.16	0.15	0.15	0.16
MgO	6.52	6.18	6.55	4.61	4.67	6.66	6.58	6.32	6.07	6.64
CaO	10.70	10.33	10.84	9.42	9.22	10.91	10.59	10.31	9.91	10.62
Na_2O	2.44	2.62	2.52	2.85	2.74	2.39	2.42	2.74	2.42	2.45
K_2O	1.89	2.10	1.94	2.08	2.08	1.82	1.92	2.51	1.93	1.94
P_2O_5	0.39	0.41	0.38	0.37	0.38	0.40	0.39	0.39	0.37	0.38
LOI	0.91	0.79	0.66	0.91	0.83	0.77	0.56	0.66	1.11	0.79

Major and trace elements by XRF (full matrix effect correction after Franzini et al. 1975) except for MgO, Na_2O and K_2O by AAS and FeO by titration. Labels of the analysed layers as in Fig. 2

Rossi et al 2000

Table 3 ^{14}C datings of the palaeosol and charred vegetation debris in trench 1

Layer	Analysed material	Conventional ^{14}C age (years B.P.±1 σ)	$\delta^{13}C_{PDB\text{-}1}$‰	Calibrated calendar age (2 σ)
l (ST66)	Organic sediment, uppermost 1 cm	1610±70	-	265–290 and 320–615 A.D.
l (ST67)	Charred material	1890±40	–28.2	55–235 A.D.
l (ST67bis)	Charred material	1750±50	–25.7	160–415 A.D.
n (ST69)	Charred material	2260±140	-	780 B.C. to 45 A.D.
p (ST84)	Charred material, uppermost 6 cm	1880±50	–24.3	45–245 A.D.
p (ST85)	Charred material, lowermost 6 cm	1860±40	–23.9	75–245 A.D.
r (ST86)	Charred material, uppermost 10 cm	2000±60	–23.8	150 B.C. to 130 A.D.
r (ST87)	Charred material, lowermost 10 cm	2000±50	–23.4	100 B.C. to 110 A.D.
w (ST92)	Charred material, uppermost 10 cm	2010±50	–22.8	115 BC to 100 A.D.
w (ST93)	Charred material, lowermost 10 cm of the trench	2200±50	–24.1	380–100 B.C.

Lables of dated layers as in Fig. 2. Datings performed by Beta Analytical Inc. (Miami, Florida). B.P. refers to a standard datum of 1950 A.D. For calibration of radiocarbon ages to calendar years see Talma and Vogel 1993

Rossi et al 2000

Vulcano, Aeolian Islands, Italy

http://www.flickr.com/search/?ss=2&w=7396920%40N05&q=vulcano&m=text

Crater at Vulcano, Aeolian Islands, Italy

http://www.flickr.com/search/?ss=2&w=7396920%40N05&q=vulcano&m=text

Fumaroles, Fosse Grande, Vulcano, November 6, 1990

http://www.ct.ingv.it/index.php?option=com_content&view=article&id=162&Itemid=211&lang=it

DeAstis et al 1997a

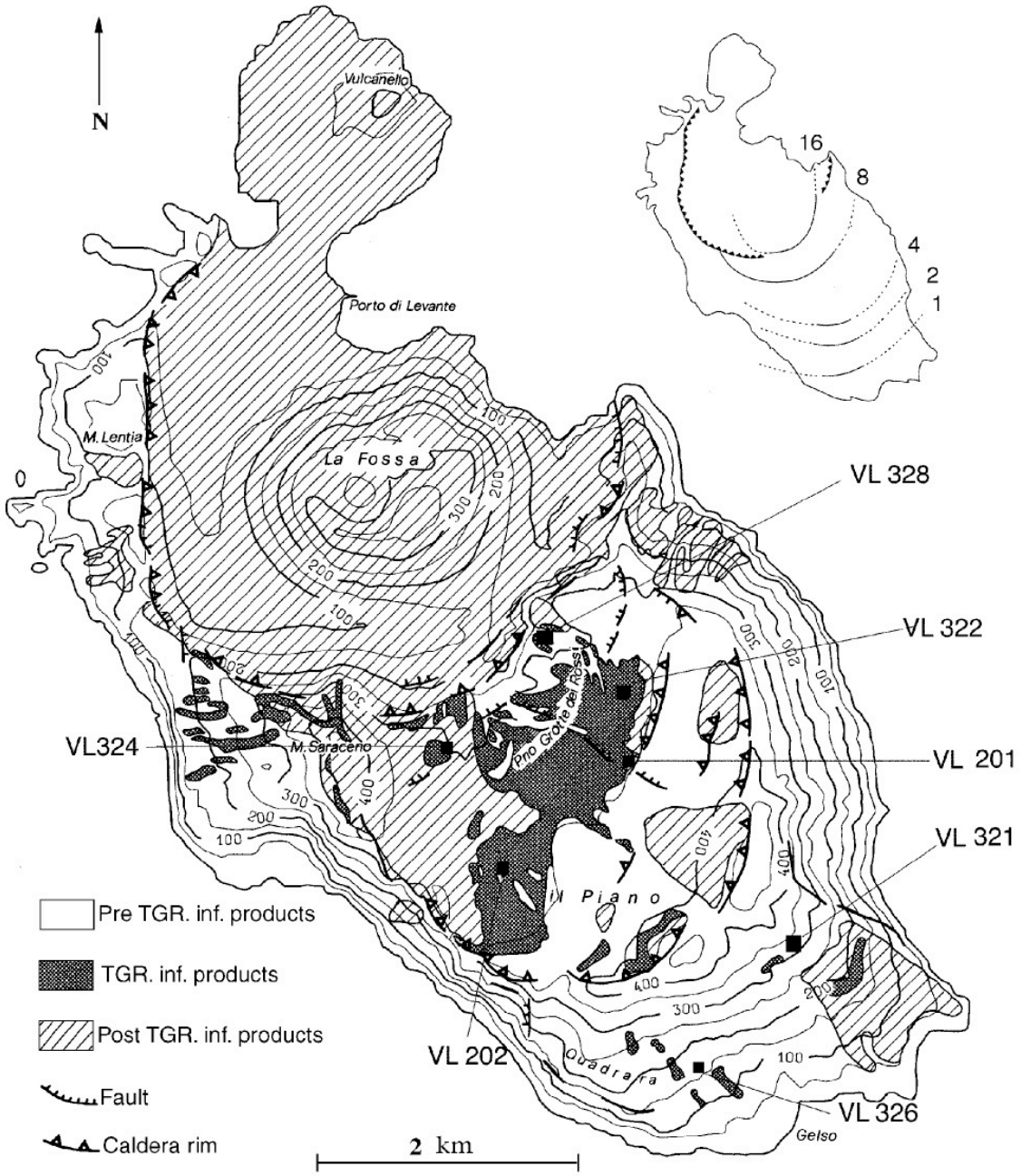

Fig. 1 Map of the dispersal area of TGR inf. deposits on Vulcano Island. Location of sections referred to in the grain-size and component analyses are reported. In the *inset* the isopach map (thickness in meters) of the TGR inferiori (TGR inf.) sequence

rallel to inclined, truncated laminae and fore-set laminae are often present.

Lithofacies-C deposits are layers centimeters to de-

Fig. 2 Erosive contact between the TGR inf. deposits (*bottom*) and the thick scoria blanket (*upper*) used as marker bed

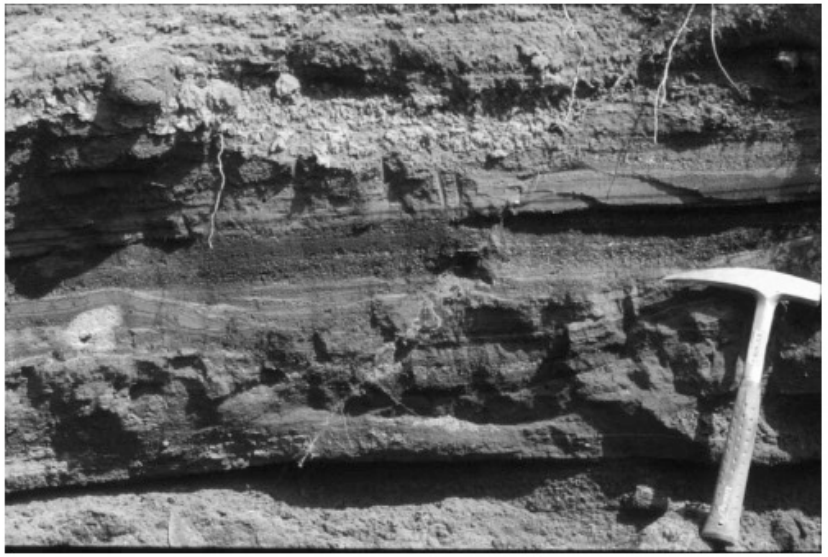

Fig. 4 Lithofacies-B laminated deposits in the Fossa caldera rim area

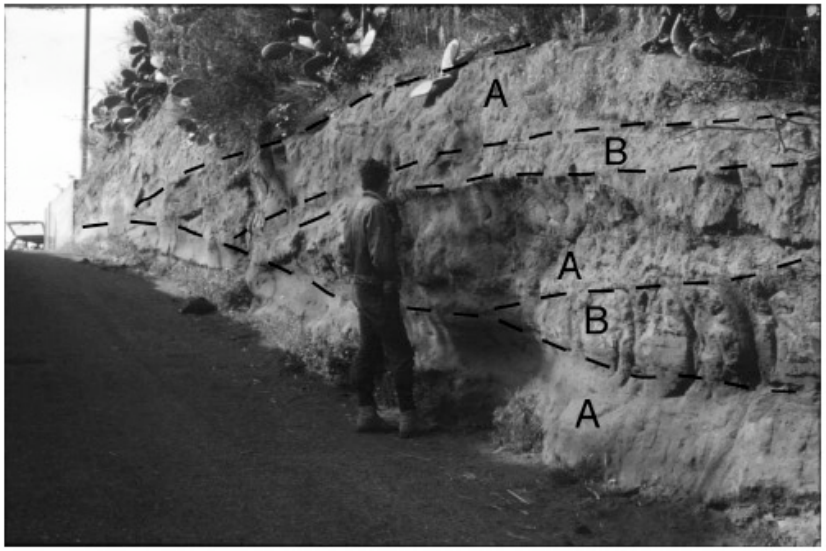

Fig. 3 TGR inf. sequence in the Piano area. *A* lithofacies-A layers with concavo-convex bedding planes; *B* lithofacies-B layers. The *dashed lines* mark the contact between different lithofacies

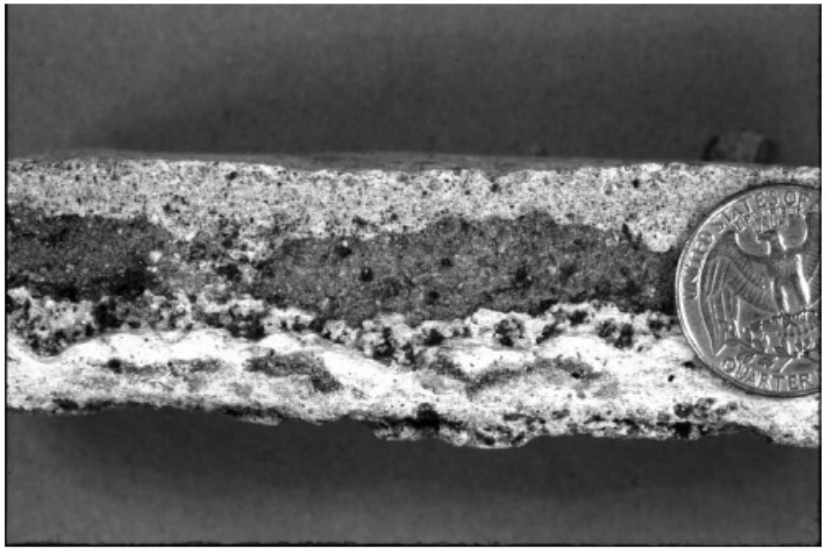

Fig. 5 Close-up of coarse (*gray*) and fine (*white*) indurated laminae of lithofacies-C deposits from the Fossa caldera rim area

DeAstis et al 1997a

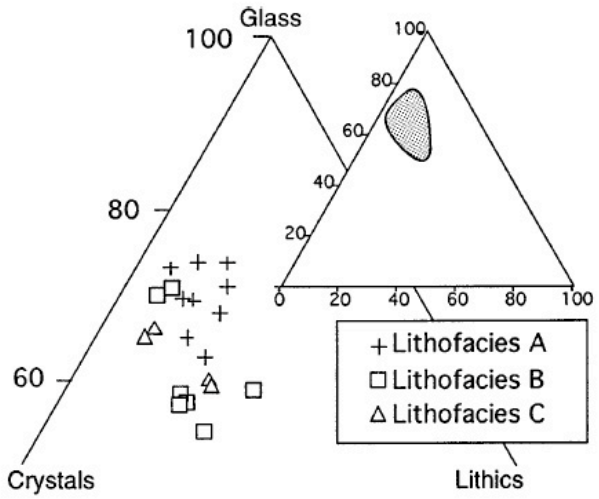

Fig. 12 Ternary diagram showing components of TGR inf. deposits

DeAstis et al 1997a

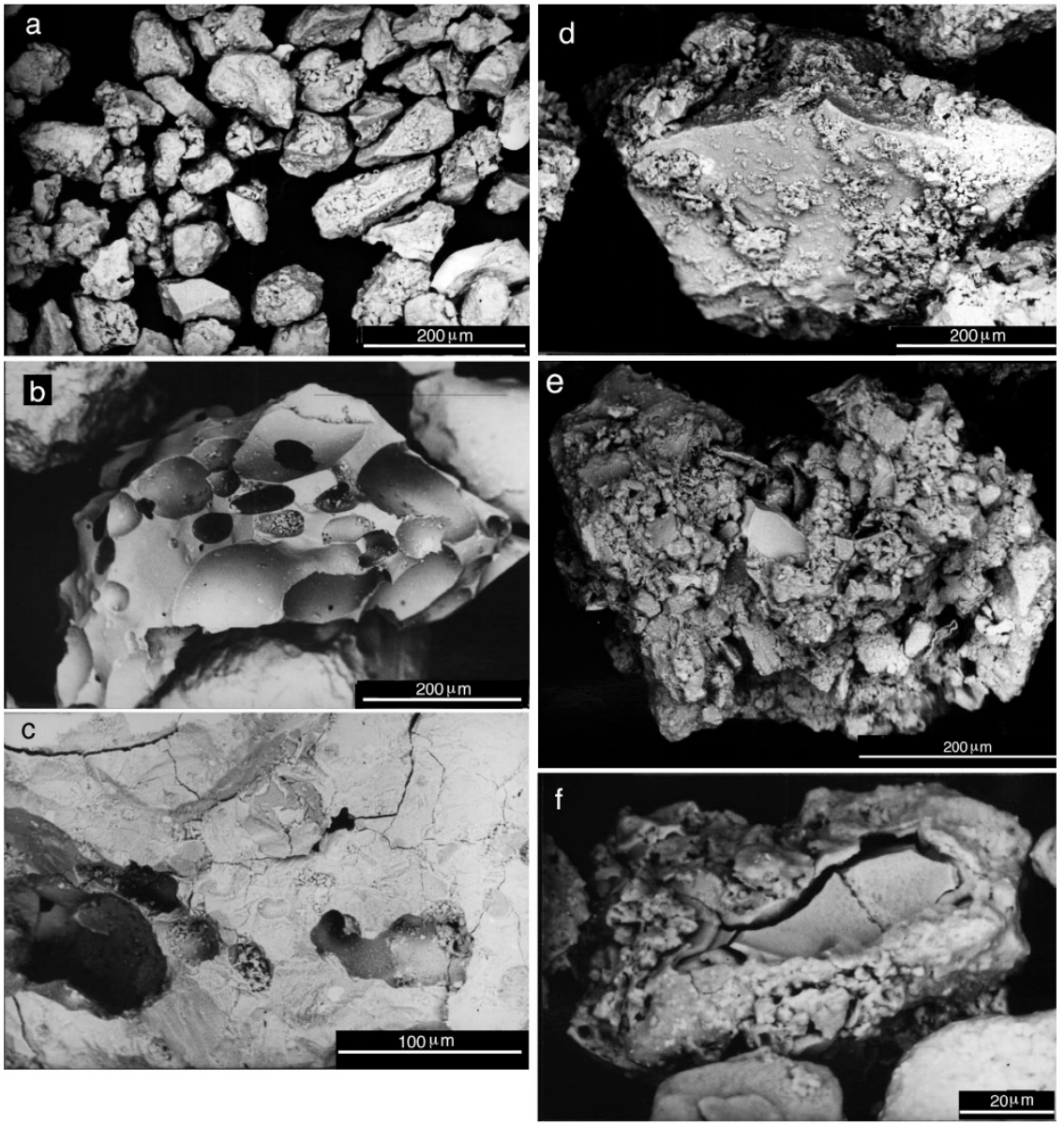

Fig. 16a–f SEM photographs of representative glass fragments from TGR inf. deposits. **a** General view of glass ash particles from a lithofacies-A sample. Particles are generally blocky and poorly vesiculated. **b** Angular highly vesiculated particle with thin vesicle walls. **c** Glass particle showing hydration cracks. **d** Blocky glass fragment with fine adhering particles on its surface. **e** Moss-like complex shape formed by blocky ash particles. **f** Glassy particle covered by "secondary skin" a few micrometers thick; in the "window" the pristine clast shows hydration cracks

to that of the coarse-ash samples. Hydration cracks are present but not common. Moss-like shapes are less common as compared with the coarse-ash fraction, since it is the aggregation of fine-ash particles that causes the formation of moss-like shapes of coarse-ash size. Moss-like shapes are also present and are more frequent in the coarse-ash fraction.

The glass particle features of both coarse- and fine-

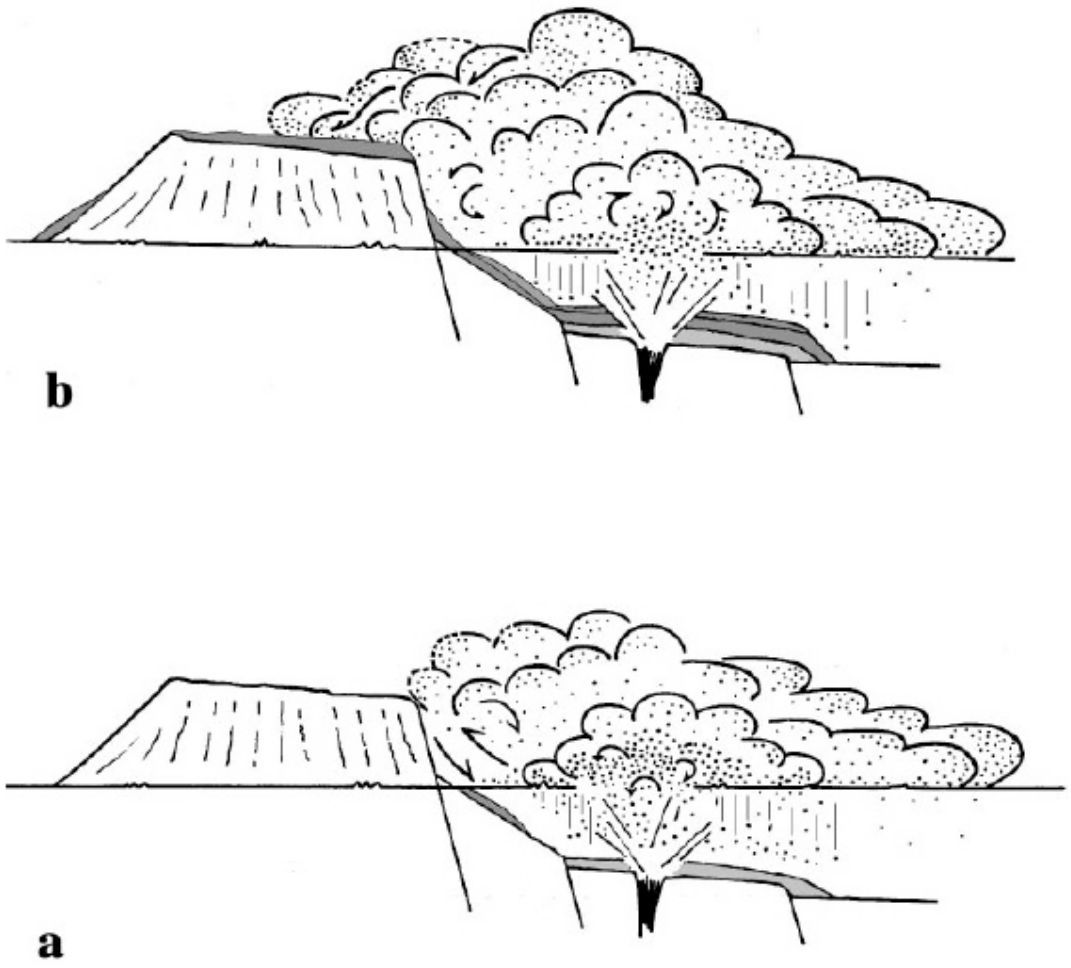

Fig. 17a, b Sketch of TGR inf. eruption model. **a** Formation of a stagnant cloud given by low energetic eruptive pulses. The energy is relatively low and the material is mostly recycled into the caldera. **b** Spreading of fresh and recycled material over the caldera rim because of more energetic pulses

De Astis et al 1997a

DeAstis et al 1997b

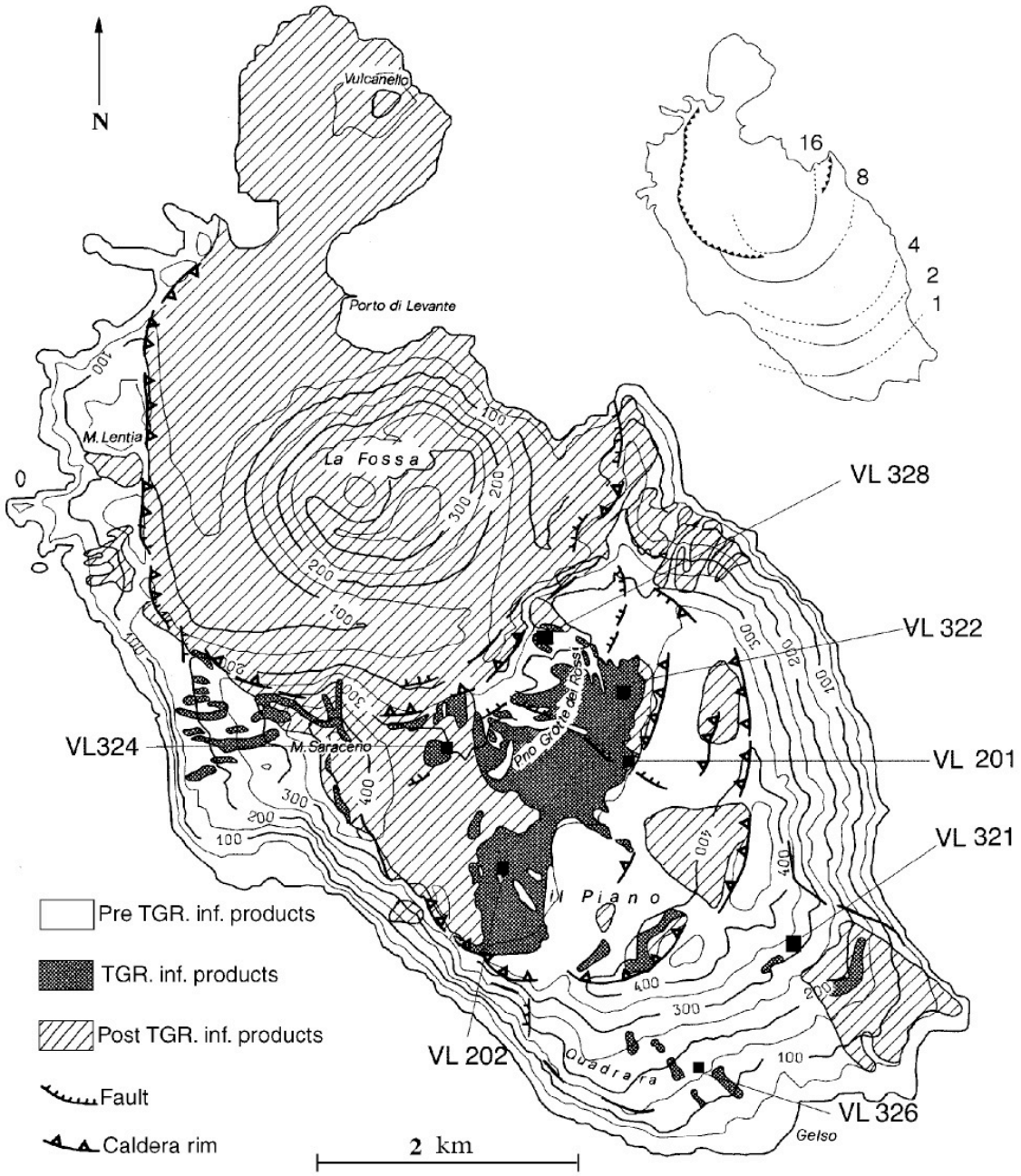

Fig. 1 Map of the dispersal area of TGR inf. deposits on Vulcano Island. Location of sections referred to in the grain-size and component analyses are reported. In the *inset* the isopach map (thickness in meters) of the TGR inferiori (TGR inf.) sequence

rallel to inclined, truncated laminae and fore-set laminae are often present.

Lithofacies-C deposits are layers centimeters to de-

Table 1. Radiometric Ages of Some Volcano-Stratigraphic Units From Vulcano

Rock Sample (Labels)	Structural Unit of Provenance	Volcano-Stratigraphic Units (VSU)	Topographic Location (AGIP Map)	K/Ar Ages,[a] ka Average	^{14}C Ages,[b] ka	Ra/Th or Th/Th Ages,[c] ka
VL 41 Z	PV	Complesso Spiaggia Lunga-Capo Secco	Spiaggia Lunga	113 ± 3.0		
VL 37 B	PV	Vulcaniti del Vulcano Primordiale (lava)	La Portella	110.5 ± 5.5		
VL 42 A	PV	Vulcaniti del Vulcano Primordiale (lava)	Grotta dell'Abate	107.5 ± 2.8		
VL 37 C	Piano Caldera	Lave leucit-tefritiche della Caldera del Piano (base)	Monte Molineddu (q. 160)	99.5 ± 7.0		
VL 40 G	Piano Caldera	Lave leucit-tefritiche della Caldera del Piano (top)	Monte Molineddu (q. 300)	78.5 ± 4.5		
VL 153/3	Piano Caldera	Lave di Timpone del Corvo	Timpone del Corvo	77.8 ± 2.1		
VL 159/5	Piano Caldera	Vulcaniti Area Monte Rosso (lava)	SW of Monte Rosso	53.7 ± 2.6		
VUL 250	Piano Caldera	Vulcaniti Area Monte Rosso (lava)	Passo del Piano	48.5 ± 2.4		
LU 1	Monte Luccia	Monte Luccia (scoriae)	north of Monte Luccia	48.5 ± 6.5		
VL 230/7	Piano Caldera	Spiaggia Lunga (scoriae)	Grotta dei Pisani			24.0 ± 5.0
VL 229/6	Piano Caldera	Quadrara (pumice)	Quadrara			21.3 ± 3.4
38 V	Lentia Complex	Lave recenti della Lentia	Monte Lentia summit	15.5 ± 1.4		
GF RO	Fossa Caldera	Lave della Roja	west of Punta Luccia	14.0 ± 6.0		
VL 139/6	Fossa Caldera	Saraceno	Monte Saraceno	8.3 ± 1.6		
VL 210 C	Fossa Caldera	TGR Sup (ash bed with carbon)	Piano di Alighieri		7680 ± 100	
LLV 124	Fossa Cone	Punte Nere (lava)	La Fossa Cone	5.5 ± 1.3		
37 D	Fossa Cone	Cicli Indeterminati (lava)	Campo Sportivo	4.6 ± 1.7		
VL 90/1	Fossa Cone	Cicli Indeterminati (scoriae)	La Fossa Cone			2.9 ± 0.4
38 S	Fossa Cone	Palizzi (pumices)	La Fossa Cone	2.2 ± 1.3		
VL 292/1	Vulcanello	Vulcanello I-II (lava)	SW of Vulcanello			1.9 ± 0.1
38 T	Fossa Cone	Palizzi (lava)	La Fossa Cone	1.6 ± 1.0		1.5 ± 0.2

PV, Primordial Vulcano. The terms of the VSU are from *De Astis* [1995].

[a]K/Ar ages are from *Frazzetta et al.* [1984, 1985] and *De Astis et al.* [1989], with analyses carried out by P. Y. Gillot (CNRS, France).

[b]Carbon 14 ages are from G. Calderoni (personal communication, 1989).

[c]Ages from the $^{226}Ra/^{230}Th$ method and $^{230}Th/^{232}Th$ versus $^{238}U/^{232}Th$ method are from A. Voltaggio et al. (personal communications, 1994–1995).

De Astis et al 1997b

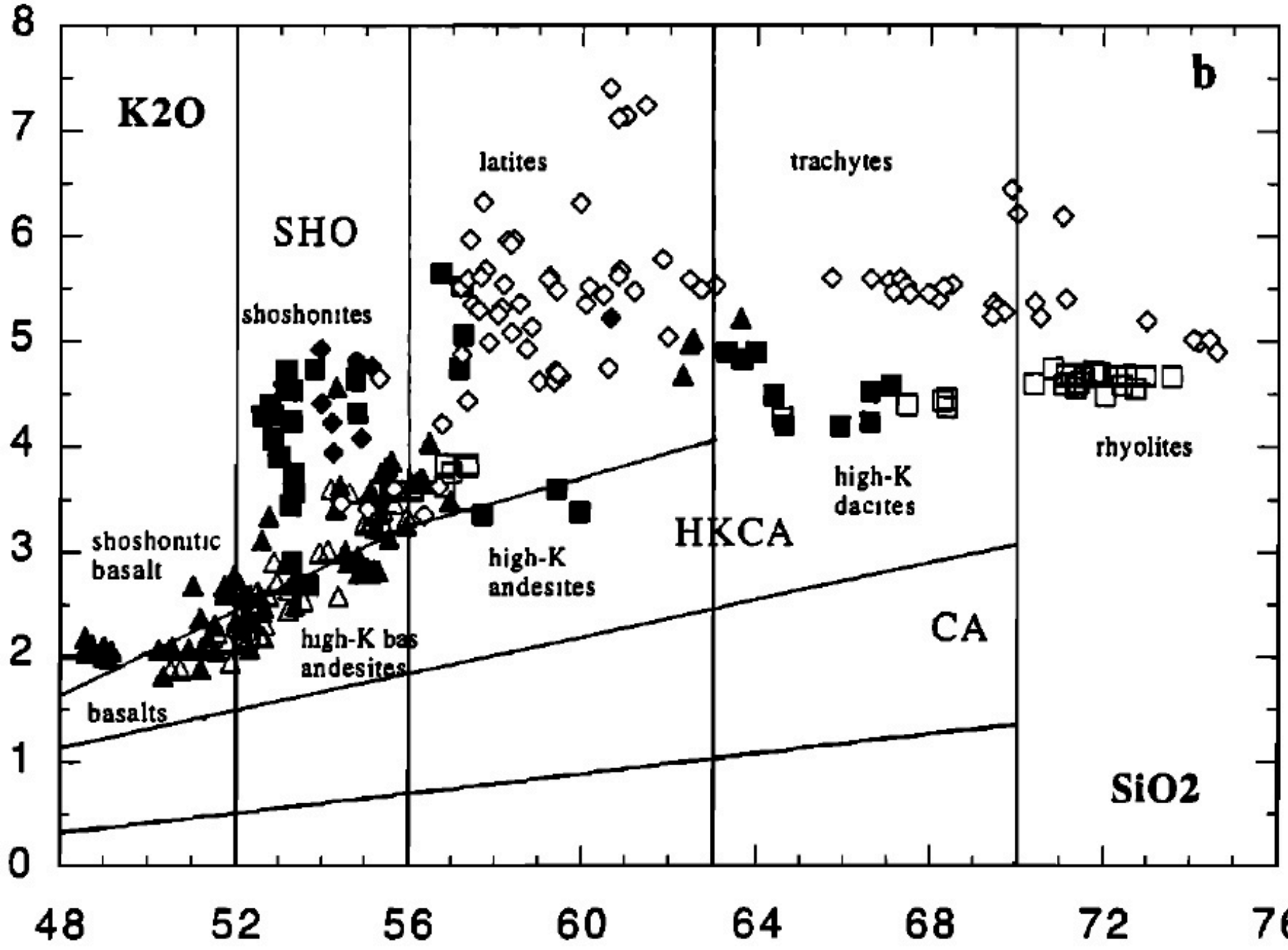

De Astis et al 1997b

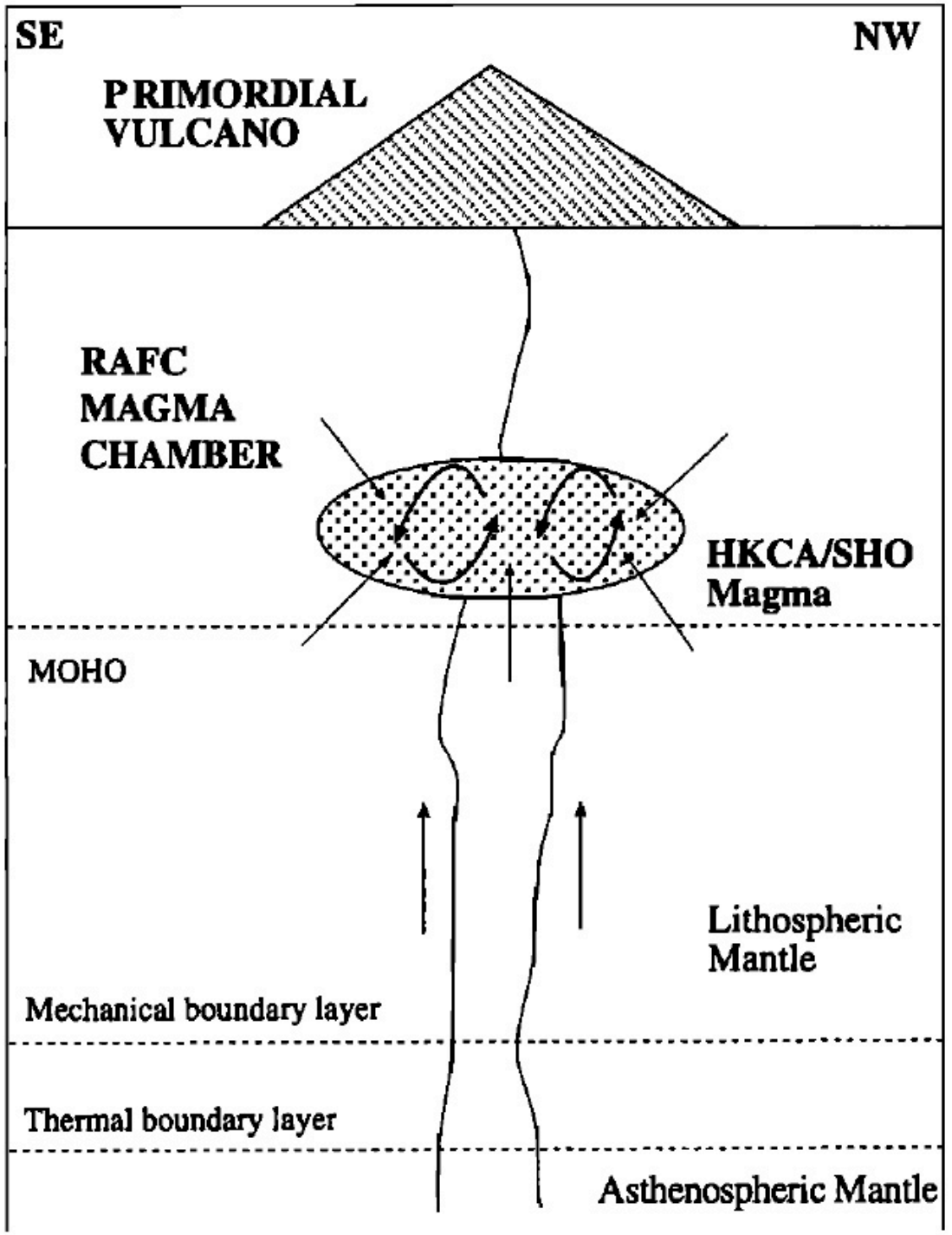

De Astis et al 1997b

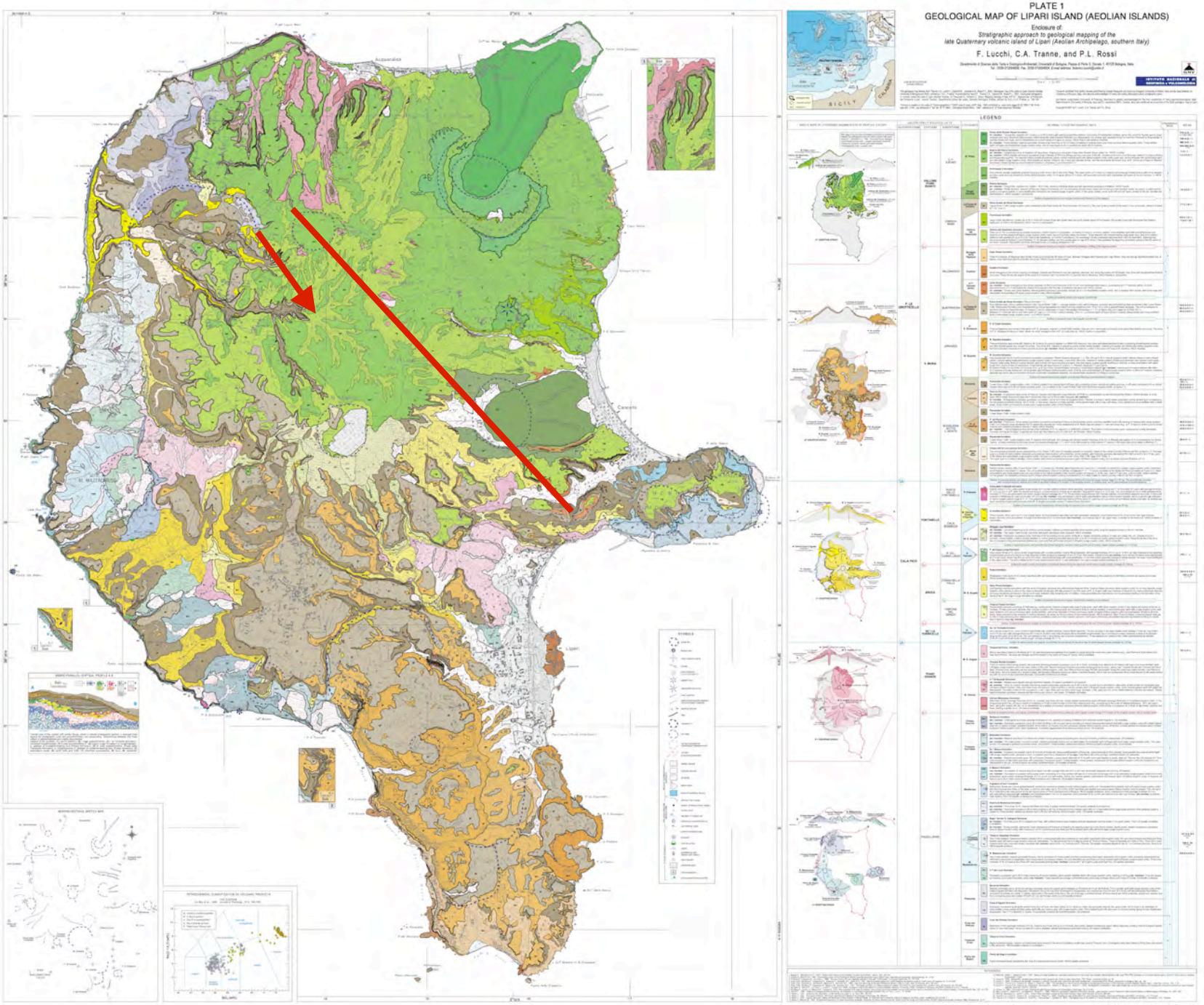

PLATE 1
GEOLOGICAL MAP OF LIPARI ISLAND (AEOLIAN ISLANDS)

Enclosure of:
Stratigraphic approach to geological mapping of the late Quaternary volcanic island of Lipari (Aeolian Archipelago, southern Italy)

F. Lucchi, C.A. Tranne, and P.L. Rossi

From Chapter 1, "Stratigraphic approach to geological mapping of the late Quaternary volcanic island of Lipari (Aeolian archipelago, southern Italy)," by Federico Lucchi, Claudio Antonio Tranne, and Piermaria Luigi Rossi.

Geological Society of America Special Paper 464
Stratigraphy and Geology of Volcanic Areas
Edited by Gianluca Groppelli and Lothar Viereck-Goette

Cortese et al 1986

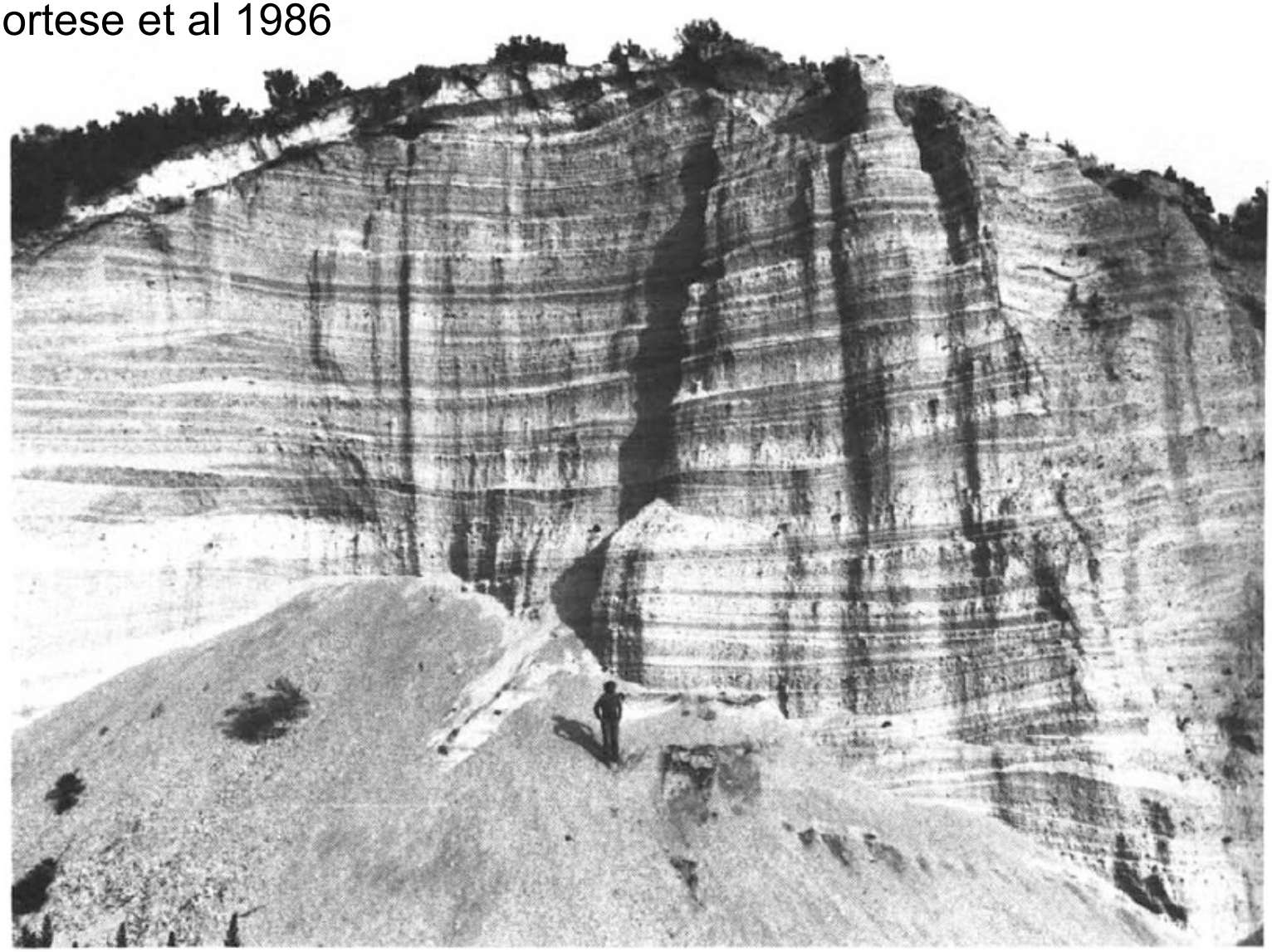

Fig. 2. Fiume Bianco. View of Gabellotto–Fiume Bianco surge sequence with predominantly wave-like bedforms. Quarry wall nearly orthogonal to transport direction. Top part of the section eroded; above the erosional surface a paleosoil horizon and conformably the white ash blanket of Monte Pilato tephra. These latter deposits show continuous mantle bedding with a uniform thickness.

Northeastern Lipari Volcanic Stratigraphy

Rocche Rosse lava flow Rocche Rosse tephra Monte Pilato tephra	Monte Pilato–Rocche Rosse VSU
Forgia Vecchia lava flow Forgia Vecchia tephra	Forgia Vecchia VSU
Pomiciazzo lava flow Gabellotto—Fiume Bianco tephra	Gabellotto—Fiume Bianco VSU
Canneto Dentro lava flow Canneto Dentro tephra	Canneto Dentro VSU

Cortese et al 1986

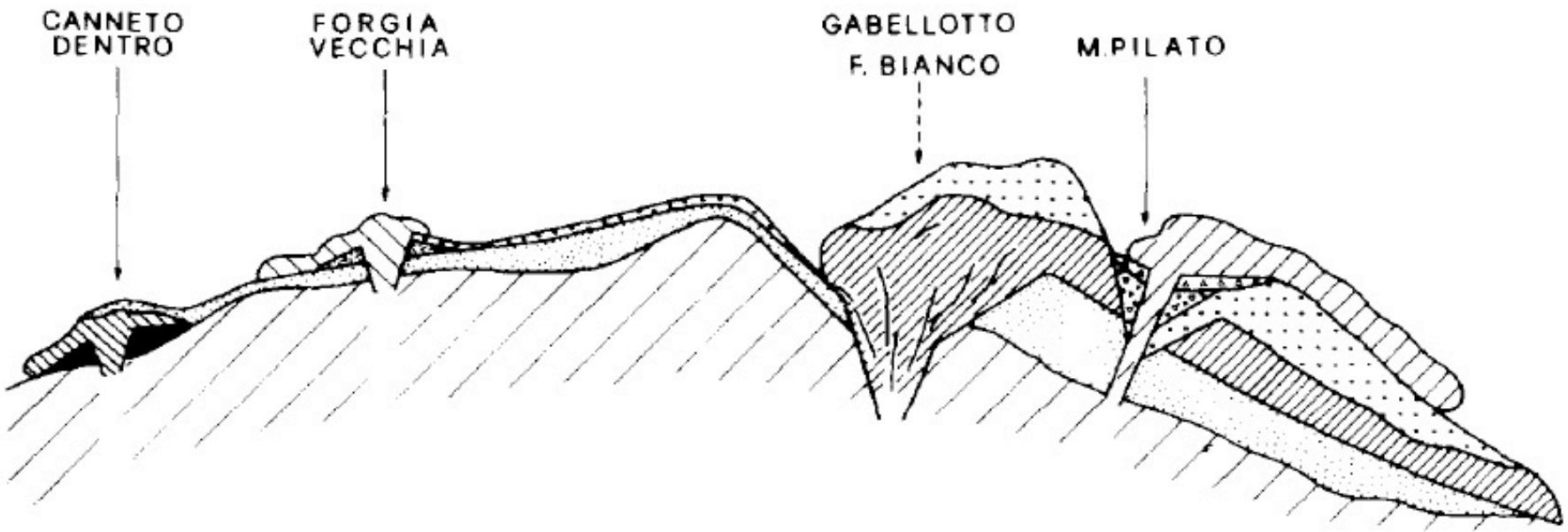

Fig. 7. Schematic cross-section illustrating the relationships between the volcano-stratigraphic units distinguished. Not to scale. Legend as in Fig. 1.

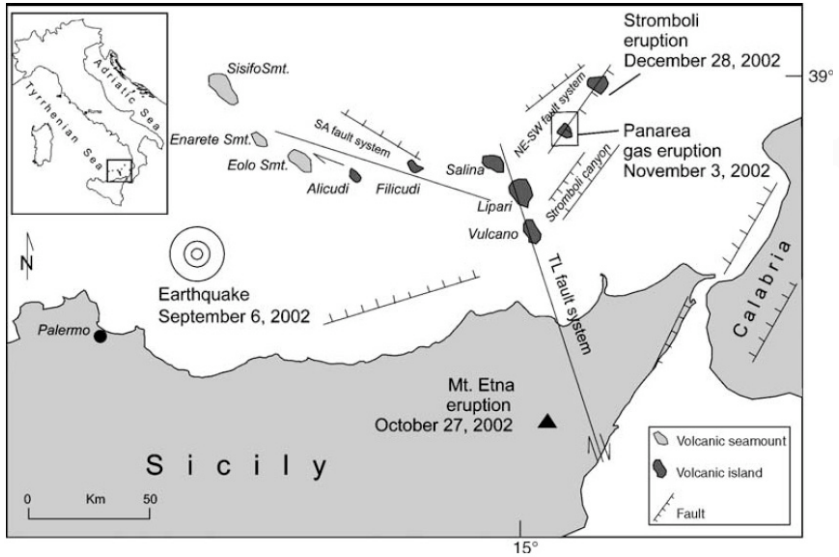

2002-03 submarine Volcanic eruption Area

(Esposito et al 2006)

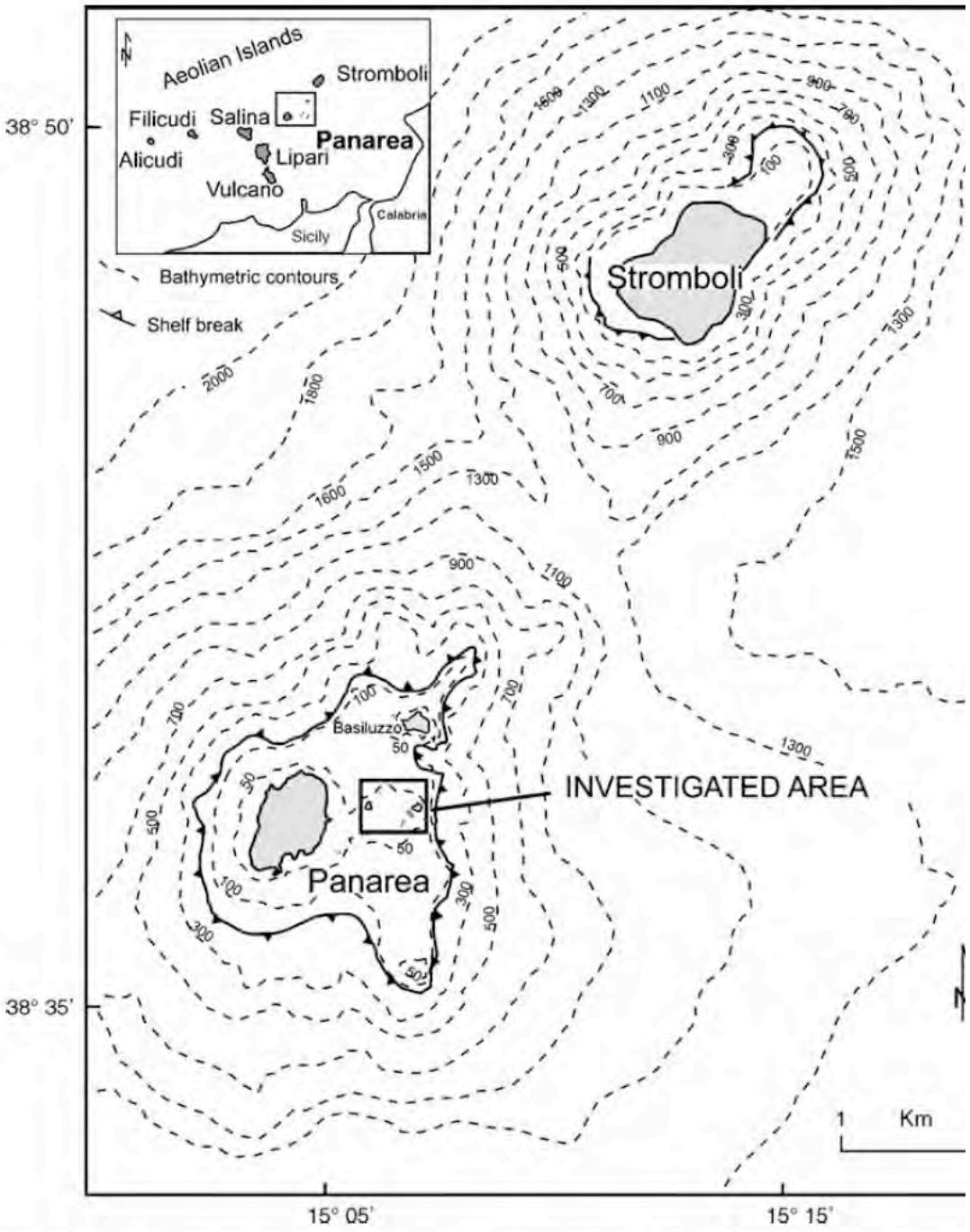

Fig. 2. Bathymetry of Panarea and Stromboli volcanoes (After Gabbianelli et al., 1

Esposito et al 2006 Bathymetric map of vent area

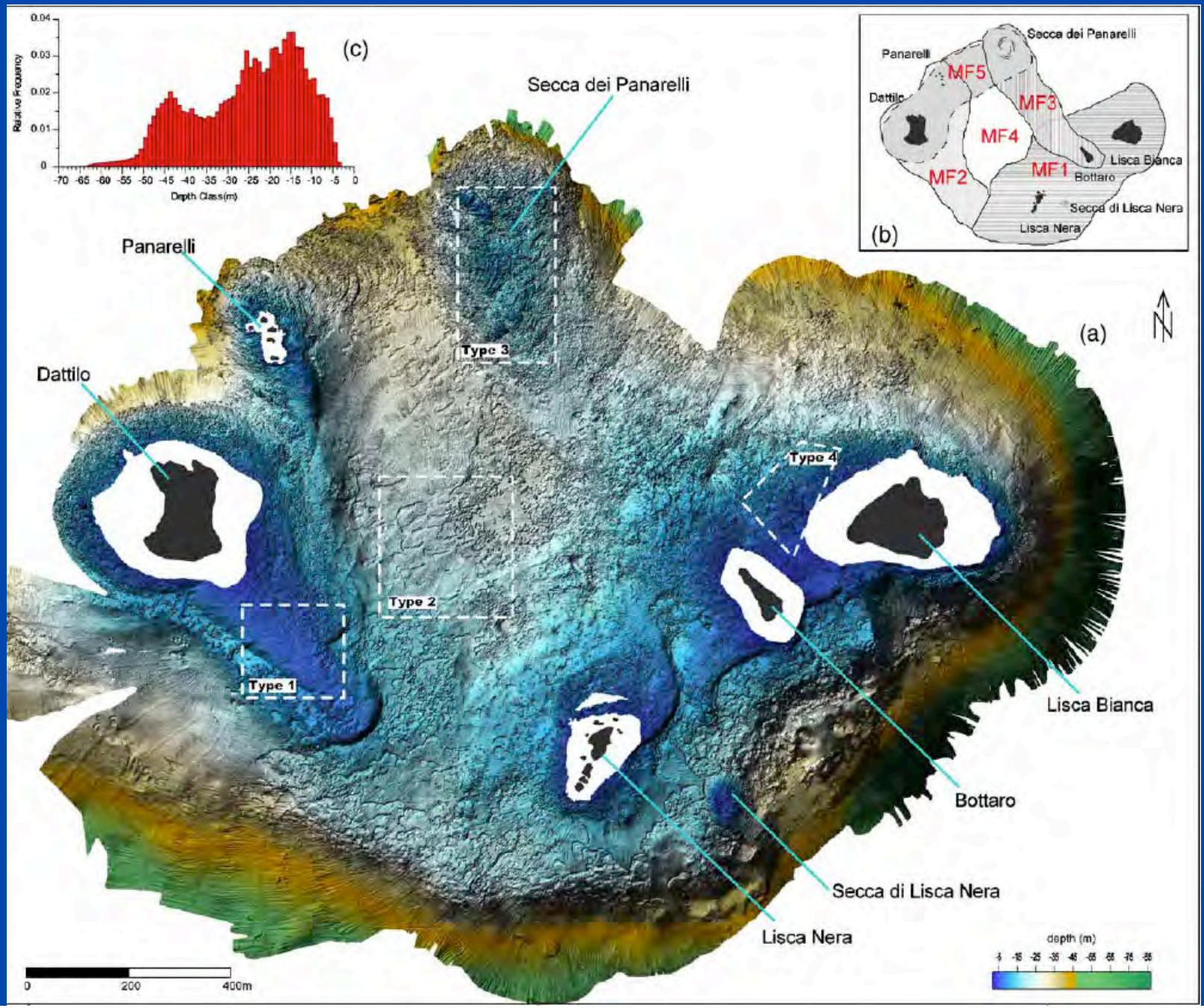

Esposito et al 2006 geologic map of vent area

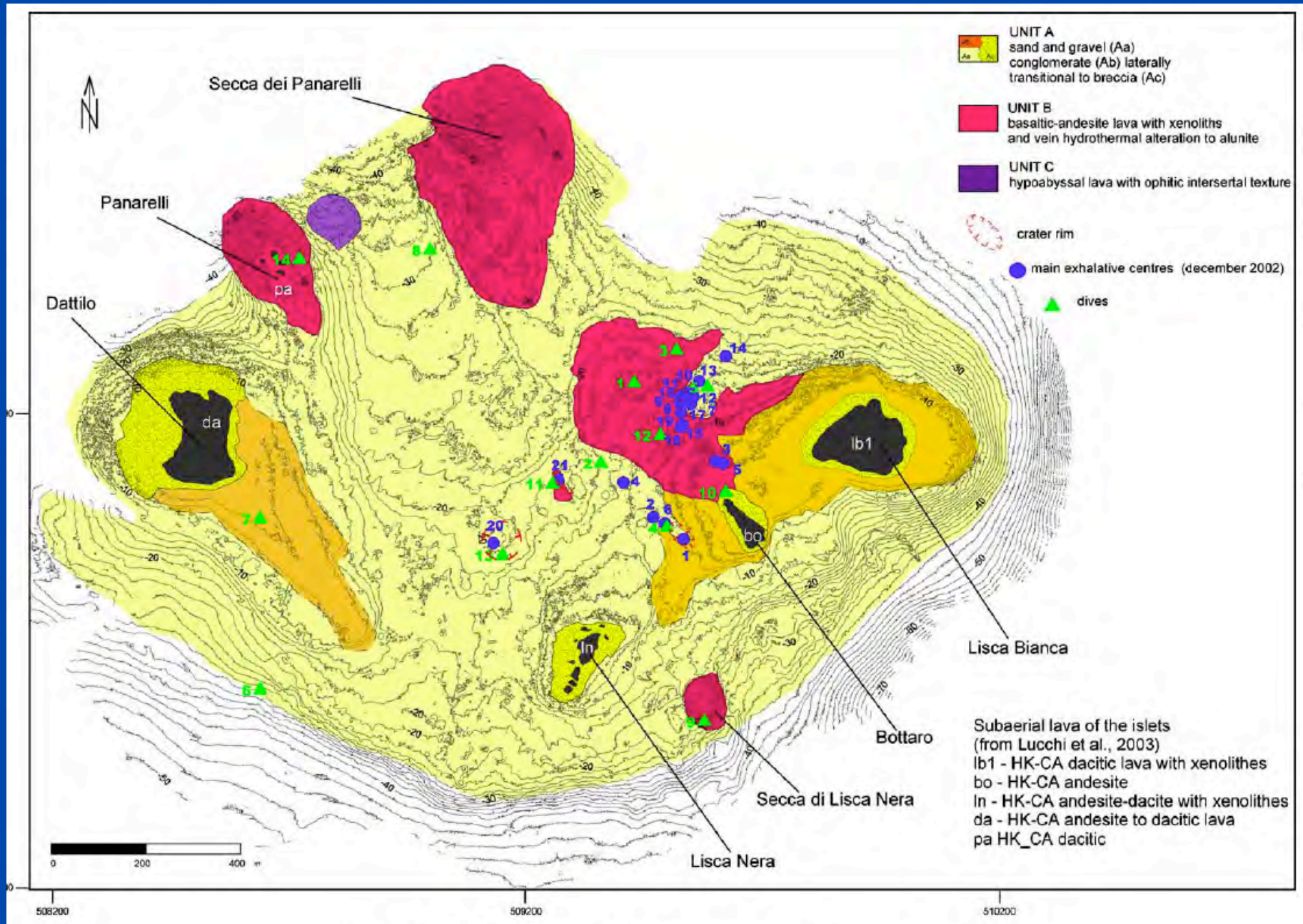

Fig. 6. Geological sketch map of the seafloor around the exhalative centres.

Table 1
Summary of geochemical characteristics of Panarea gas emissions

CO_2	H_2S	H_2	N_2	He	Ar	CH_4	CO	Flux	Authors
92.5–99%	0.1–6.5%	5 ppm		8 ppm		0.1 ppm	0.1	9×10^6 l/d total area	Italiano and Nuccio, 1991
98.8–95.4%	0.5–4.0	10–30 ppm	0.52–1.1			6–585 ppb	10–65ppb	100.000	Calanchi et al., 1995
97.3–98.4%	1–2.4%	0.001–0.12% Increased	0.2–0.5%	0.0008–0.001% Increased by 1000 times	0.0008–0.0054%	0.0004–0.001%	0.0001–0.0008%		Chiodini et al., 2003 Caramanna et al., 2003
96.6–98.6%	1.2–2.2%	0.071–0.12%	0.2–0.5%	0.0008–0.001%	0.0008–0.0054%	0.0004–0.001%	0.0001–0.0008%	10^9 l/d	Caliro et al., 2004

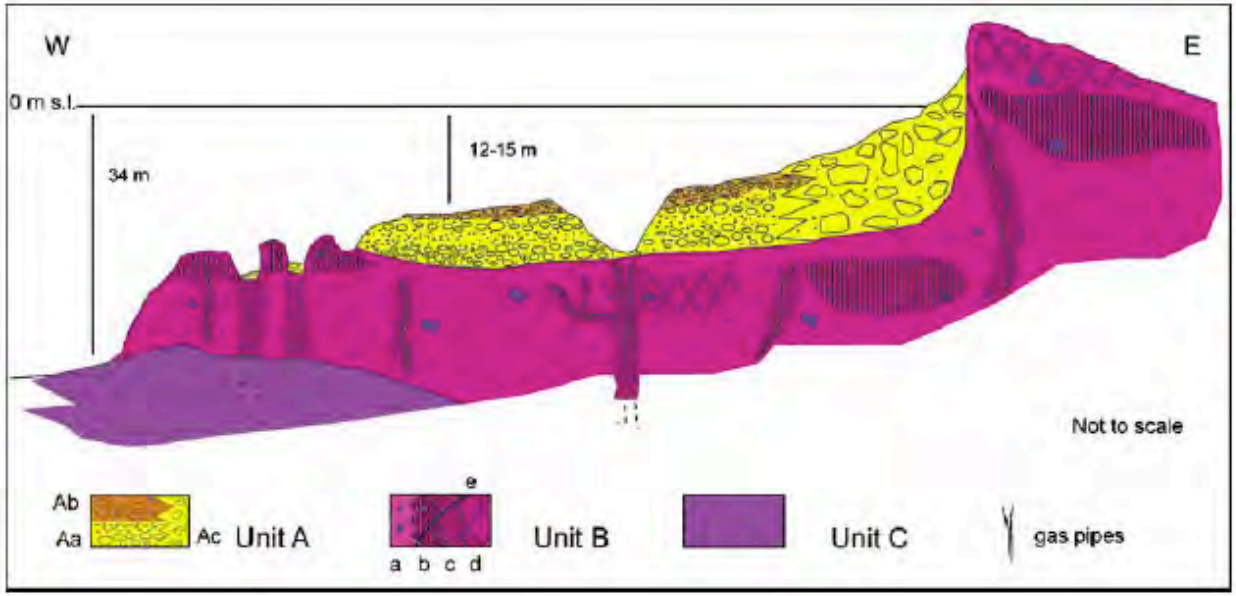

Fig. 7. Stratigraphic relationships of units of the seafloor, showing the different lithofacies. Unit C highly crystalline andesite lava; Unit B basaltic–andesite to andesite porphyric lava with xenolites ((a) coherent facies, (b) flow banded facies, (c) hydrothermally altered facies, (d) jigsaw-fit breccia facies, (e) alunite veins); Unit A (Aa sand and gravel, Ab, conglomerate, Ac breccia).

Esposito et al 2006: Gas emissions data & sea floor stratigraphy

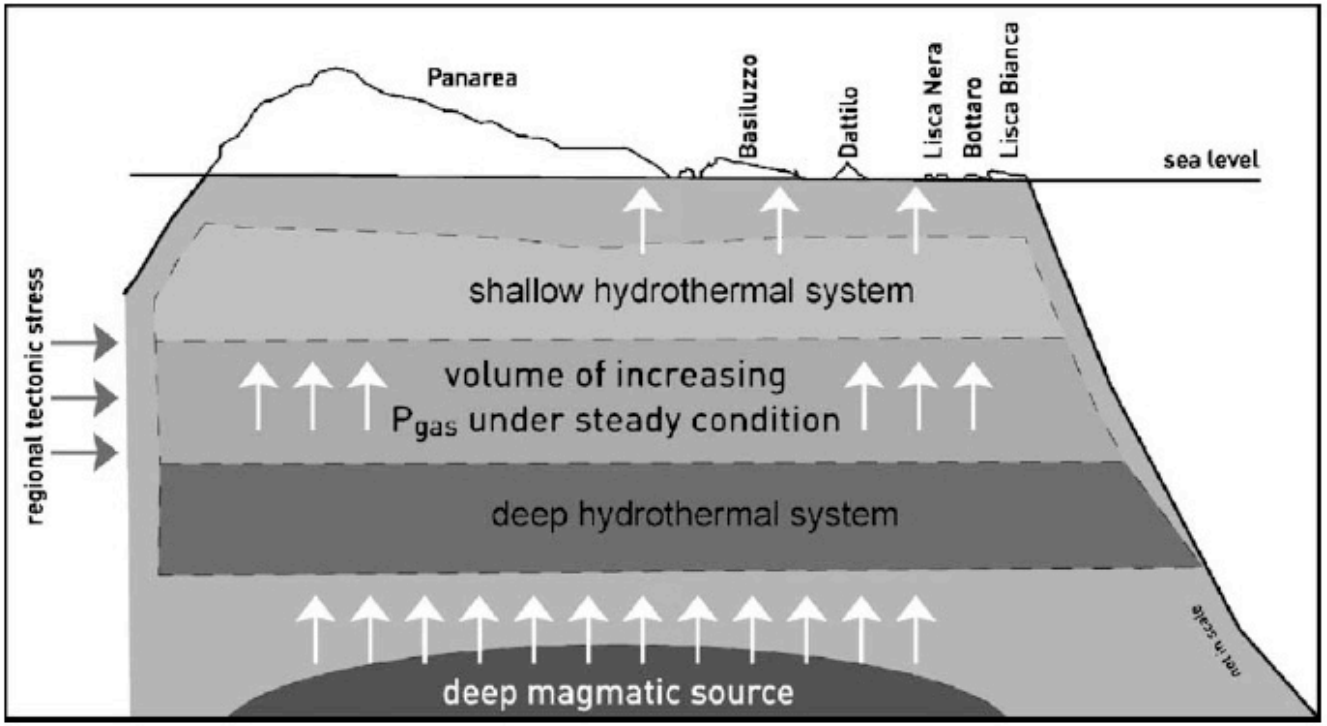

Fig. 11. Model explaining the November 2002 Panarea gas eruptions in terms of accumulation at depth of pressurised gas from the steady or quasi-steady release of gas from a deep magmatic source, likely a cooling magma body and the periodic release of the overpressure when the tensile strength of the overlying rocks is overcome either by the increased internal pressure or by external changes of the tectonic stress.

Esposito et al 2006

Stromboli Eruptions

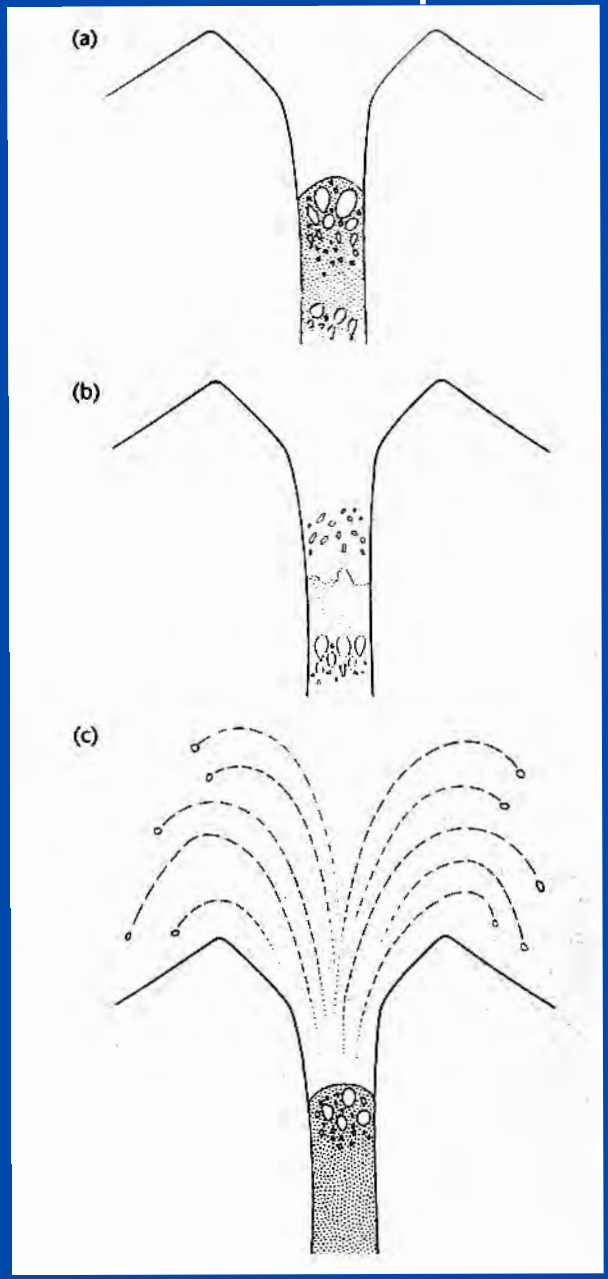

Short lived eruptions, marked by pauses.

Erupts basaltic pyroclastic fragments.

Does not produce an eruptive column.

Francis & Oppenheimer 2004

Vulcanian Eruptions

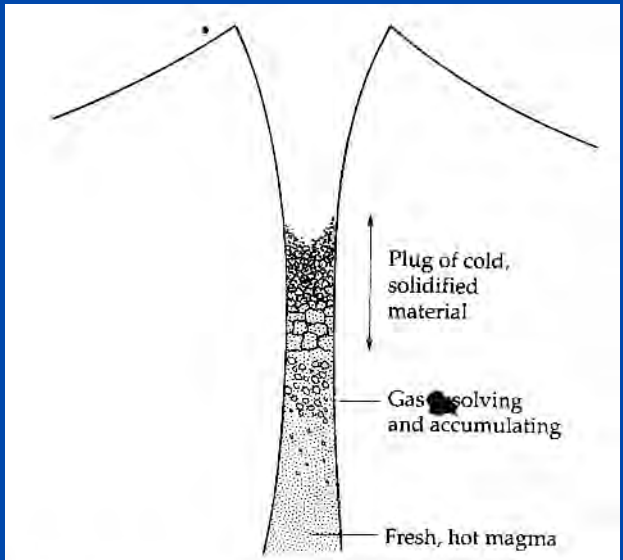

Fig. 5.16 Many vulcanian eruptions are thought to involve a plug of solidified material in the throat of a vent, due to build-up of volatile pressure in deeper-seated magma.

Francis & Oppenheimer 2004

Brief, explosive eruptions.

Small magnitude.

Eruption columns may reach 20 km.

Violent, producing small fragments including volcanic ash.

May be the first phase of a prolonged eruption.

Andesite magma is often present

Volcanic Magnitude

$$M = \log_{10} m - 7$$

M = magnitude

M = mass of tephra or lava

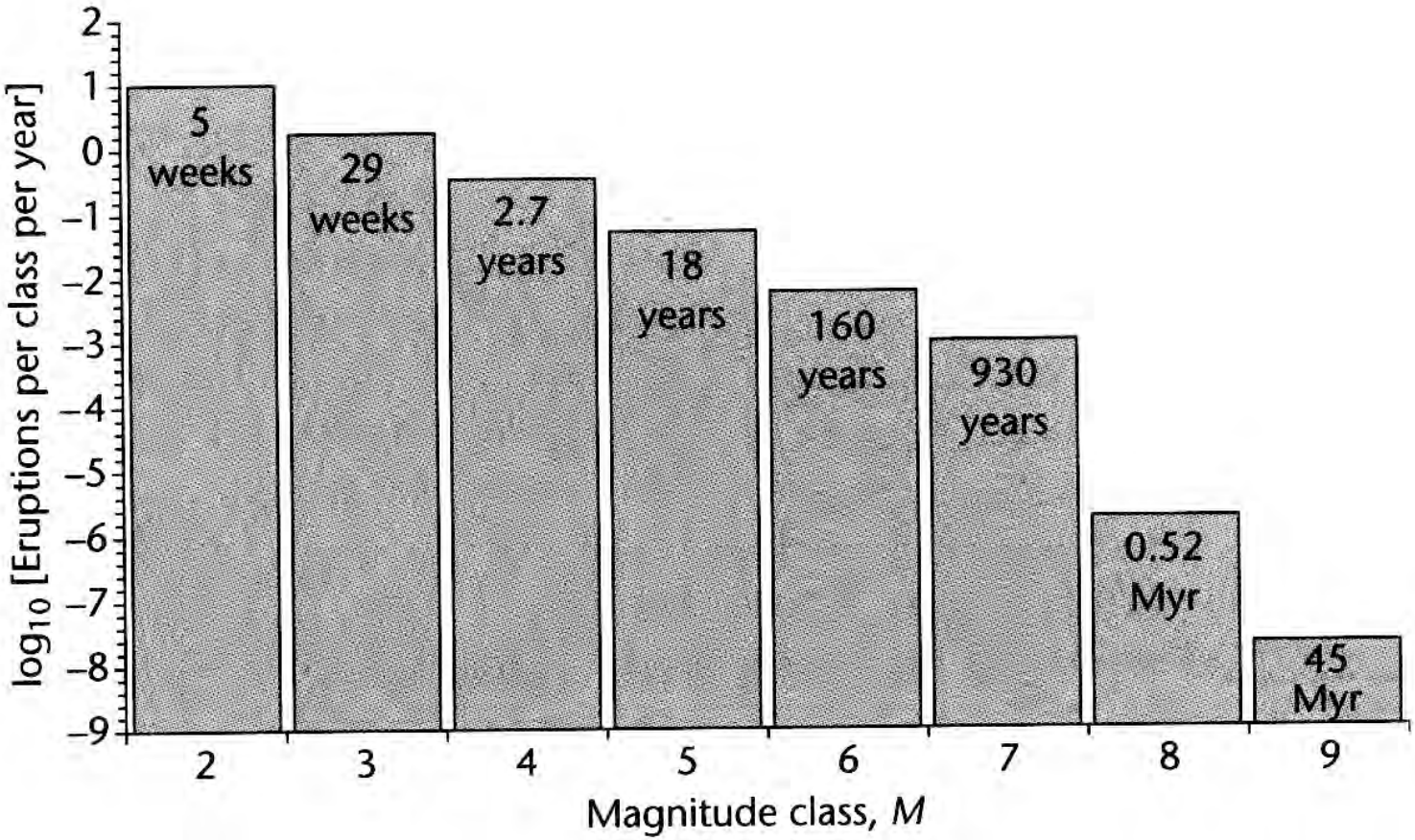

Fig. 5.5 Magnitude–frequency plot for subaerial volcanic eruptions based on records for last 300 yr for $2 \leq M < 6$; last 2 kyr for $6 \leq M < 8$; and for all known 'super-eruptions' of the past 45 Myr for $M \geq 8$. Note that extrapolation of the more or less reliable record for the past 300 years or even the last 2 kyr, to estimate the frequency of very large eruptions ($M \geq 8$), would result in a significant over-estimation of the their recurrence. The only $M = 9$ eruption in this compilation is the Fish Canyon Tuff eruption associated with La Garita caldera in the United States (Section 11.7), the implied frequency of magnitude 9 events should therefore be regarded

Data from D. Pyle and B. Mason

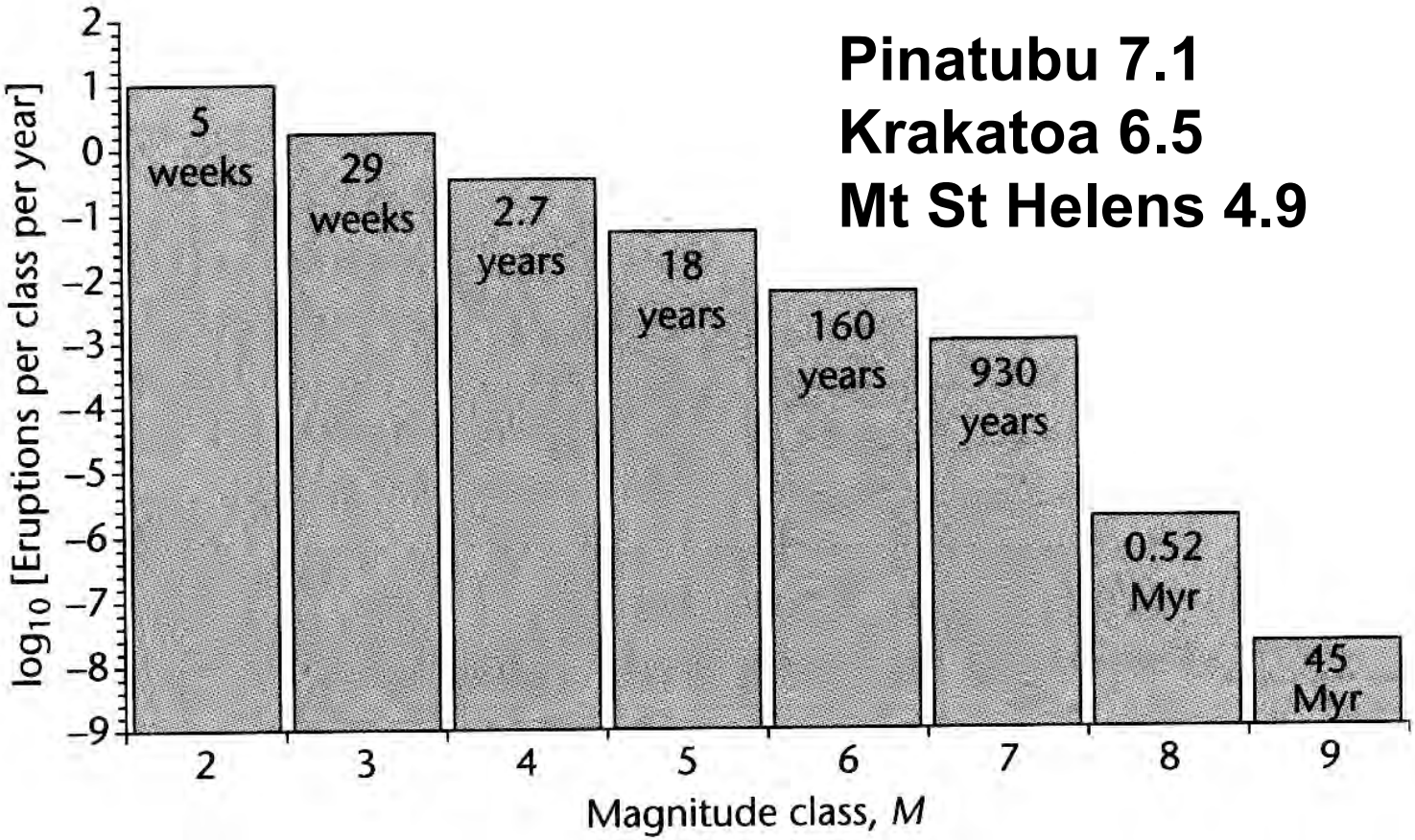

Fig. 5.5 Magnitude–frequency plot for subaerial volcanic eruptions based on records for last 300 yr for $2 \leq M < 6$; last 2 kyr for $6 \leq M < 8$; and for all known 'super-eruptions' of the past 45 Myr for $M \geq 8$. Note that extrapolation of the more or less reliable record for the past 300 years or even the last 2 kyr, to estimate the frequency of very large eruptions ($M \geq 8$), would result in a significant over-estimation of the their recurrence. The only $M = 9$ eruption in this compilation is the Fish Canyon Tuff eruption associated with La Garita caldera in the United States (Section 11.7), the implied frequency of magnitude 9 events should therefore be regarded

Data from D. Pyle and B. Mason

A Simplified Volcanic Activity Classification

- Diffuse degassing and fumeroles
- Hawaiian eruptions
- Lava lakes
- Strombolian eruptions
- Vulcanian eruptions
- Visuvian or sub-plinian eruptions (M‹4)
- Plinian eruptions (M=4+)
- Pelean eruptions
- Hydrovolcanic eruptions

Viscosity of Diverse Materials

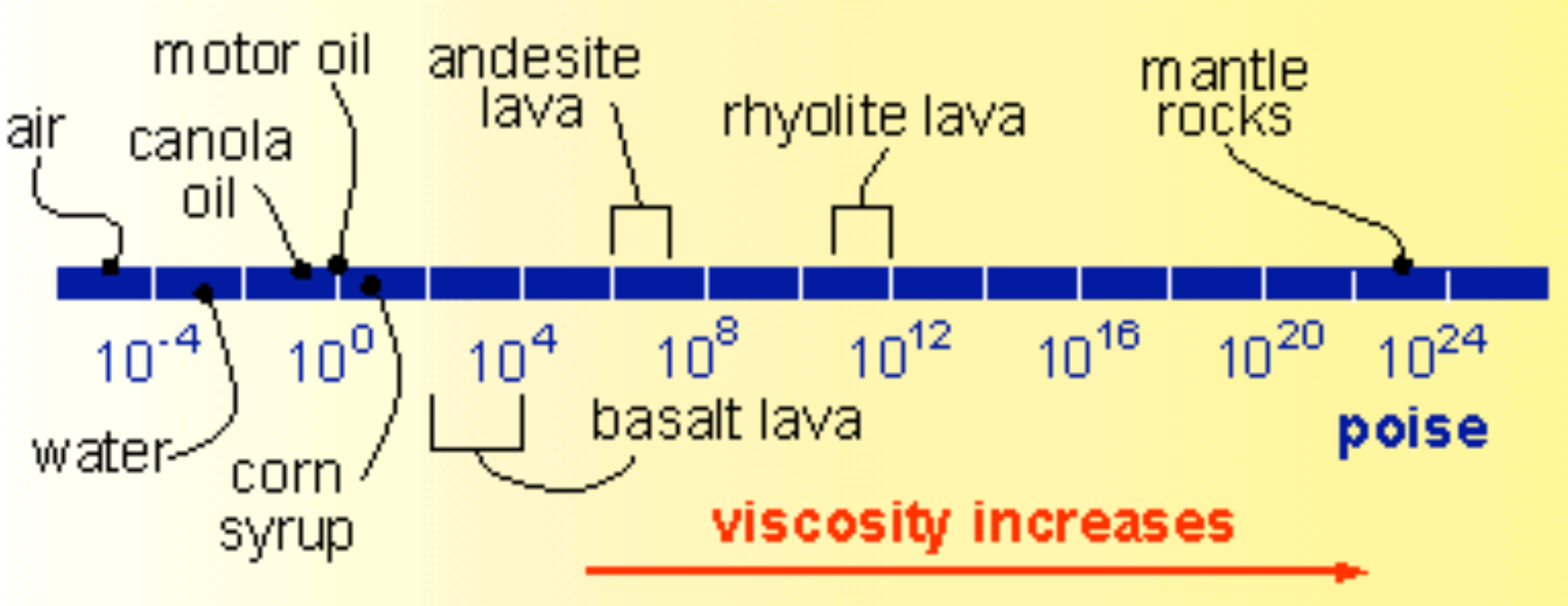

http://www.earth.northwestern.edu/people/seth/107/Rocks/Image24.gif

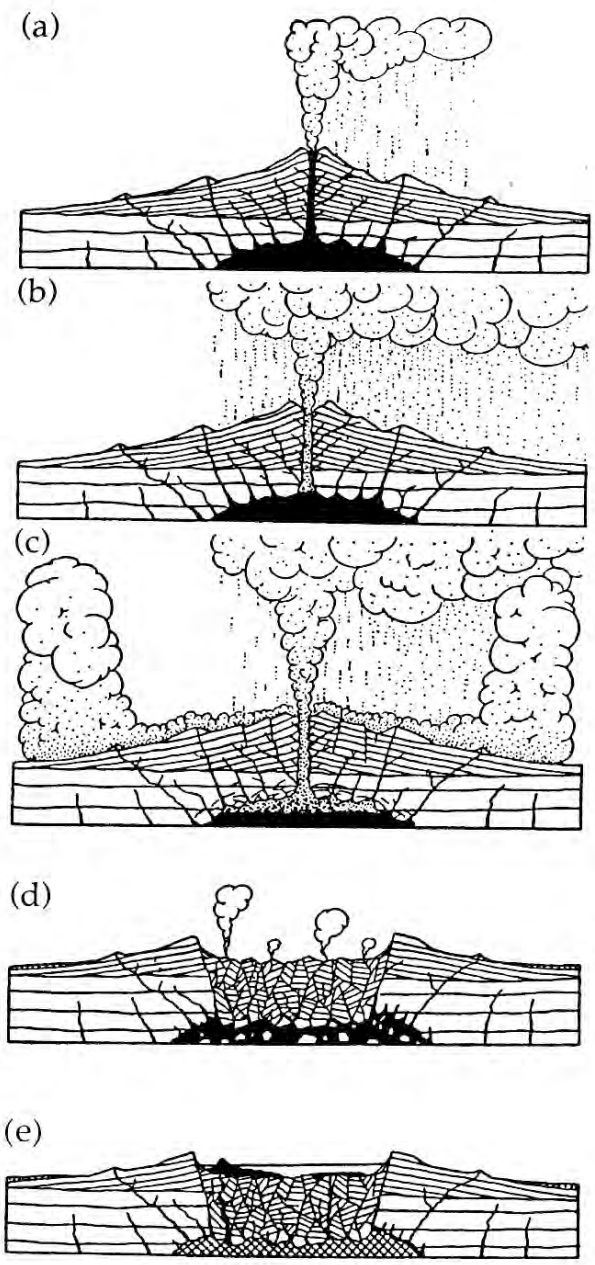

Fig. 11.5 Howel Williams's classic diagrams illustrating the formation of Crater Lake caldera Oregon [13]. His original

Formation of Crater Lake Howell Williams (1941)

(reproduced in Francis and Oppenheimer 2004)

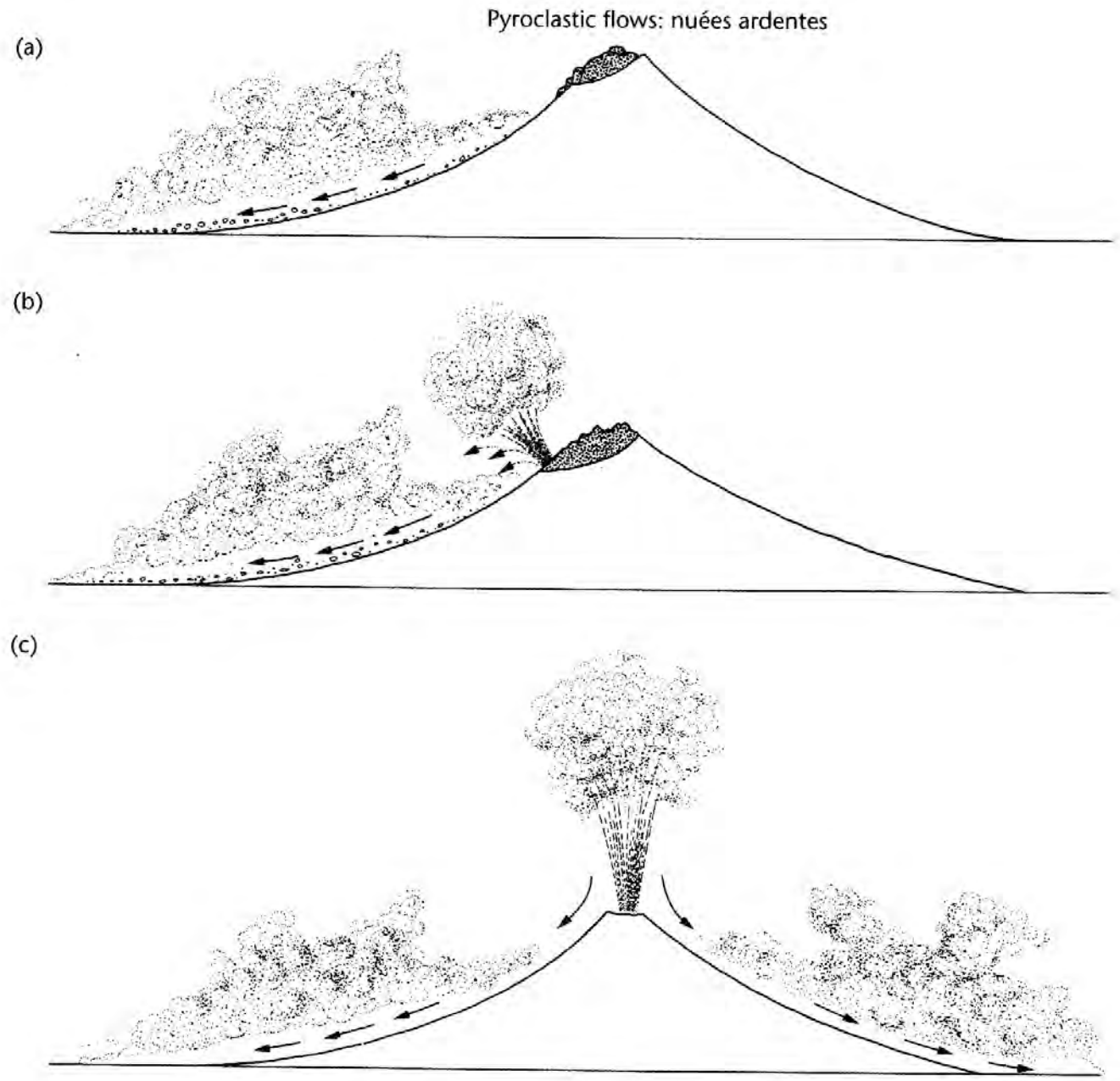

Fig. 9.7 Three common mechanisms for generating PDCs. (a) Simple gravitational collapse of a growing lava dome or flow on a volcano (merapi type). (b) Explosive disruption of growing lava dome (peléean type). (c) Collapse from eruption column (soufrière type).

Francis and Oppenheimer 2004)

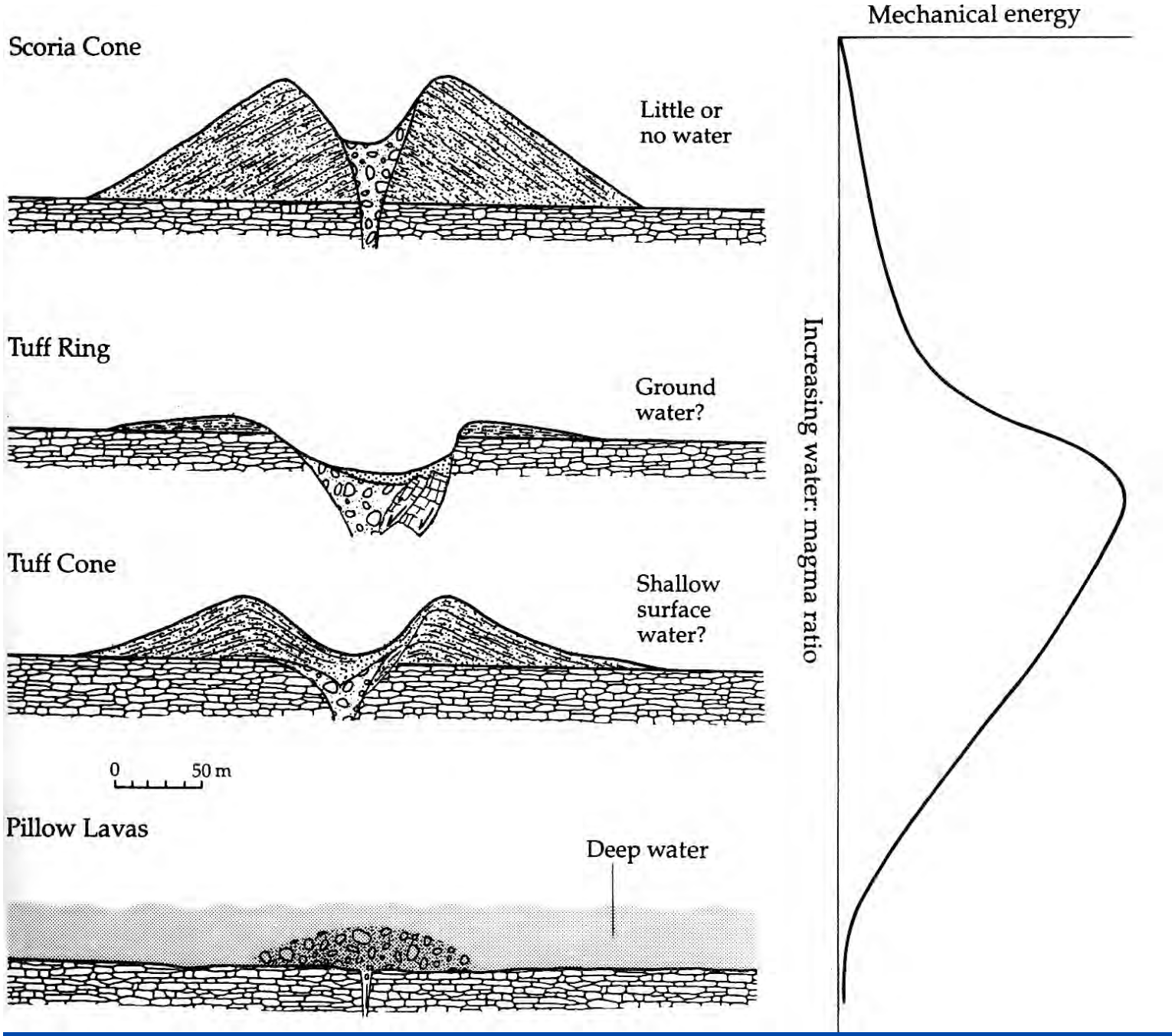

Francis and Oppenheimer 2004)

Impact of water on small basaltic eruptions

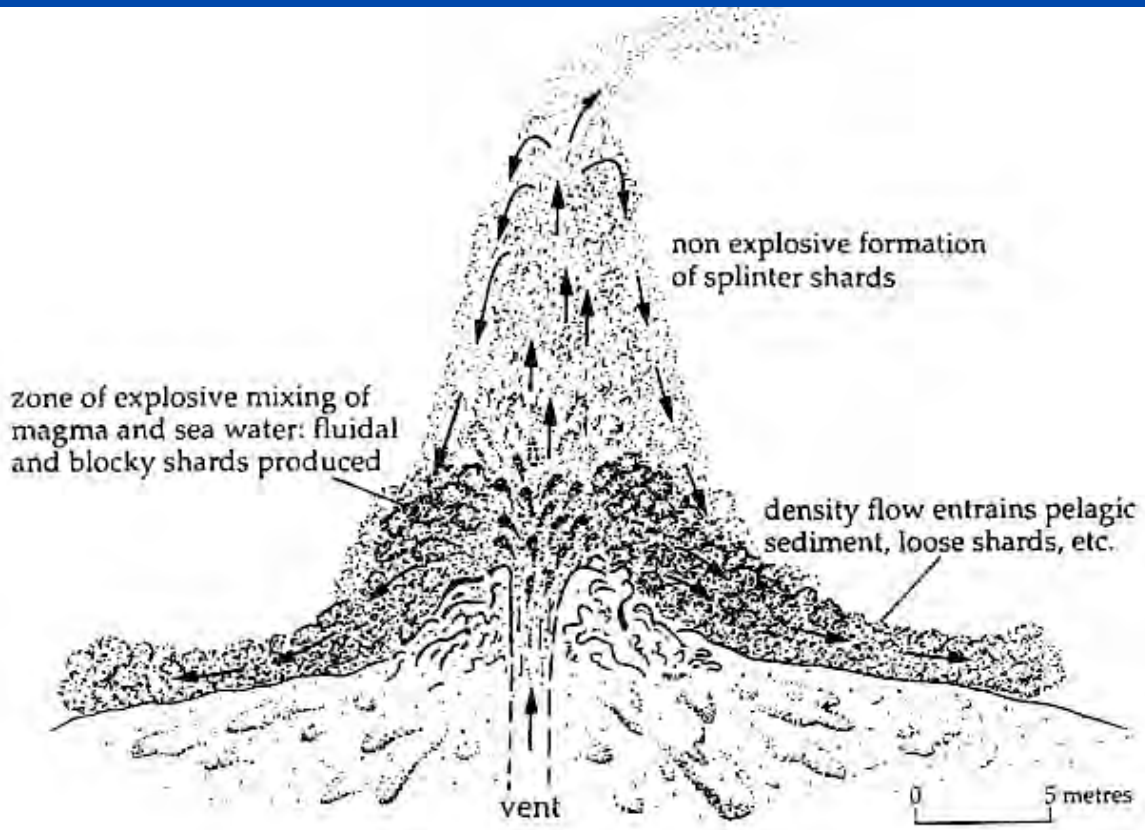

Fig. 14.15 Direct formation of hyaloclastites in deep water, where lava fountains up through the sea floor. Hyaloclastite outcrops formed in this way were found on six seamount volcanoes near the East Pacific Rise at depths between 1240 and 2500 m. From [25].

Francis and Oppenheimer 2004)

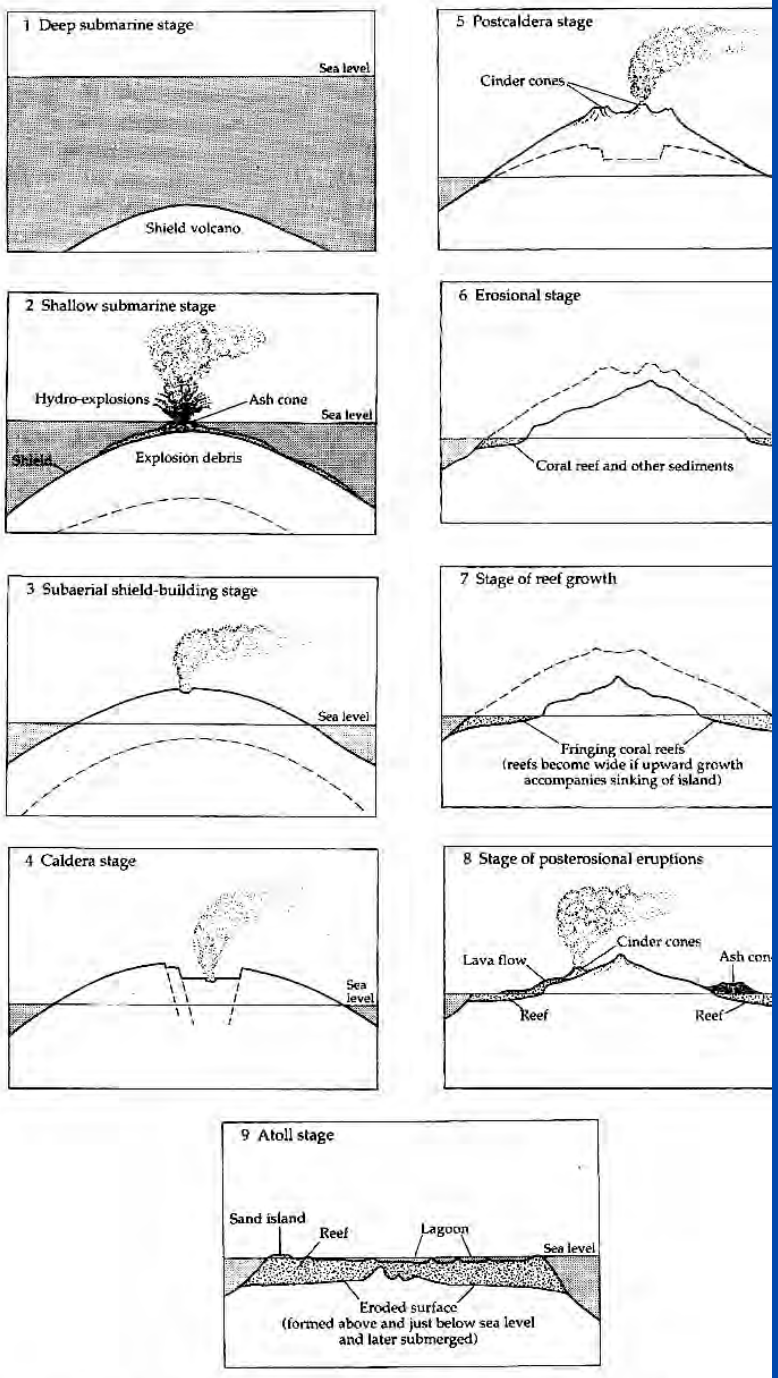

Fig. 13.17 Stages in the morphological evolution of Hawaiian shield volcanoes. After [18].

Francis and Oppenheimer 2004)